Published in final edited form as:
J Comp Neurol. 2010 April 1; 518(7): 1133–1155. doi:10.1002/cne.22268.

Immunocytochemical Localization of Synaptic Proteins to Photoreceptor Synapses of *Drosophila melanogaster*

Yoshitaka Hamanaka[1,3] and **Ian A. Meinertzhagen**[1,2,3,*]

[1]Department of Psychology, Life Sciences Centre, Dalhousie University, Halifax, Nova Scotia, Canada B3H 4J1

[2]Department of Biology, Life Sciences Centre, Dalhousie University, Halifax, Nova Scotia, Canada B3H 4J1

[3]Neuroscience Institute, Life Sciences Centre, Dalhousie University, Halifax, Nova Scotia, Canada B3H 4J1

Abstract

The location of proteins that contribute to synaptic function has been widely studied in vertebrate synapses, far more than at model synapses of the genetically manipulable fruit fly, *Drosophila melanogaster* . *Drosophila* photoreceptor terminals have been extensively exploited to characterize the actions of synaptic genes, and their distinct and repetitive synaptic ultrastructure is anatomically well suited for such studies. Synaptic release sites include a bipartite T-bar ribbon, comprising a platform surmounting a pedestal. So far, little is known about the composition and precise location of proteins at either the T-bar ribbon or its associated synaptic organelles, knowledge of which is required to understand many details of synaptic function. We studied the localization of candidate proteins to pre- or postsynaptic organelles, by using immuno-electron microscopy with the pre-embedding method, after first validating immunolabeling by confocal microscopy. We used monoclonal antibodies against Bruchpilot, epidermal growth factor receptor pathway substrate clone 15 (EPS-15), and cysteine string protein (CSP), all raised against a fly head homogenate, as well as sea urchin kinesin (antibody SUK4) and Discs large (DLG). All these antibodies labeled distinct synaptic structures in photoreceptor terminals in the first optic neuropil, the lamina, as did rabbit anti-DPAK (*Drosophila* p21 activated kinase) and anti-Dynamin. Validating reports from light microscopy, immunoreactivity to Bruchpilot localized to the edge of the platform, and immunoreactivity to SUK4 localized to the pedestal of the T-bar ribbon. Anti-DLG recognized the photoreceptor head of capitate projections, invaginating organelles from surrounding glia. For synaptic vesicles, immunoreactivity to EPS-15 localized to sites of endocytosis, and anti-CSP labeled vesicles lying close to the T-bar ribbon. These results provide markers for synaptic sites, and a basis for further functional studies.

*CORRESPONDENCE TO: I.A. Meinertzhagen, Department of Psychology, Life Sciences Centre, Dalhousie University, Halifax, Nova Scotia, Canada B3H 4J1. iam@dal.ca.

Additional Supporting Information may be found in the online version of this article.

INDEXING TERMS

synaptic vesicle; lamina; ribbon synapse; capitate projection; histamine

The release of neurotransmitters in the brain is both rapid and highly focal, mediated by exocytosis at the active zones of synaptic terminals (recent reviews: Verhage and Toonen, 2007; Rizo and Rosenmund, 2008). Vesicle exocytosis in turn involves a cascade of protein-protein interactions (Südhof, 1995; Rizo and Rosenmund, 2008) that form part of the synaptic vesicle cycle (Südhof, 2004). The cycle is centered on the highly differentiated structure of the active zone (Burns and Augustine, 1995), reported from conventional electron microscopy (EM) many years ago (e.g., Akert et al., 1972) or more recently at higher resolution by means of EM tomography (e.g., Lenzi et al., 1999; Harlow et al., 2001). The architecture of the active zone shows many common features at the synapses of different nervous systems, and is matched to the rate of neurotransmitter release (Zhai and Bellen, 2004). General features include a meshwork of cytoskeleton that encompasses a cumulus of synaptic vesicles and an electron-dense cytomatrix at the active zone (CAZ) that lines the presynaptic plasma membrane (Peters et al., 1991; Garner et al., 2000; Gundelfinger and tom Dieck, 2000; De Camilli et al., 2001).

Electron-dense projections of various shapes at the pre-synaptic site have been the subject of many reports (Zhai and Bellen, 2004), and these are especially conspicuous at ribbon synapses of the vertebrate retina, where an electron-dense organelle is specialized for vesicle shedding (Sterling and Matthews, 2005). In the fruit fly *Drosophila melanogaster* , an electron-dense presynaptic ribbon, T-shaped in cross section, occurs at many synapses in the central nervous system (CNS) (Prokop and Meinertzhagen, 2006), and all peripheral synapses of the compound eye's photoreceptor terminals (Meinertzhagen and O'Neil, 1991; Meinertzhagen and Sorra, 2001). These T-shaped presynaptic projections have for many years been referred to as presynaptic ribbons, by comparison with the organelles in vertebrate photoreceptors (Meinertzhagen, 1993). To unify the terminology for these organelles at two model synapses in *Drosophila* , neuromuscular junctions (NMJs), and photoreceptor synapses, we refer to them as *T-bar ribbons* (Prokop and Meinertzhagen, 2006).

At mammalian synapses, docking and priming of synaptic vesicles occur at the CAZ, prior to vesicle shedding and neurotransmitter release (Garner et al., 2000). Recent studies have identified and functionally characterized the protein components of the CAZ at conventional synapses (reviewed in Rosenmund et al., 2003; Zhai and Bellen, 2004; Schoch and Gundelfinger, 2006), and at the ribbon complex of vertebrate rods (tom Dieck et al., 2005). Although knowledge of the complete protein composition of the CAZ remains incomplete, the list includes: Munc13-1 (Brose et al., 1995), RIMs (Wang et al., 1997, 2000), ERC/ CAST (Ohtsuka et al., 2002; Wang et al., 2002), Piccolo/ Aczonin, and Bassoon (Cases-Langhoff et al., 1996; tom Dieck et al., 1998; Wang et al., 1999). These are all thought to be essential for the formation and function of synapses, and the proper assembly of presynaptic structures at the active zone.

The CAZ protein CAST (Ohtsuka et al., 2002; Wang et al., 2002) forms a ternary complex with RIM1 and Munc13-1 by directly binding RIM1 (Ohtsuka et al., 2002). Moreover, CAST directly binds not only to RIM1 but also to Bassoon and Piccolo, and is involved in neurotransmitter release by directly binding these CAZ proteins (Takao-Rikitsu et al., 2004). The gene *bruchpilot* , which codes for a *Drosophila* homologue of CAST, has recently been cloned (Wagh et al., 2006). Its product, Bruchpilot (BRP) has been localized to the T-bar ribbons of *Drosophila* NMJs (Kittel et al., 2006). It therefore seems plausible that other homologues of mammalian synaptic proteins may also localize to *Drosophila* presynaptic sites.

The differential localization of CAZ and other proteins has been widely studied at mammalian synapses (tom Dieck et al., 2005; Deguchi-Tawarada et al., 2006), but little is known about their localization at the synapses of other nervous systems, especially those in *Drosophila* , in which the opportunity to study synaptic mutants is particularly propitious. *Drosophila* is the most obvious model species because of the diversity of synaptic proteins, the close conservation of those for the neurotransmitter release, and availability of the many transposon insertion sites near the corresponding genes (Lloyd et al., 2000), which allow the ready generation of synaptic mutants. These genetic advantages are allied to the distinctive pre-synaptic ultrastructure of *Drosophila* synapses, especially the bipartite T-bar ribbon (Prokop and Meinertzhagen, 2006). The latter comprises a platform, which surmounts a pedestal (Fröhlich, 1985; Meinertzhagen and O'Neil, 1991).

Many studies report the expression of *Drosophila* CAZ and other synaptic proteins using confocal microscopy, especially at larval NMJs, an easily accessible and readily visualized glutamatergic synapse (Budnik and Ruiz-Canada, 2007). There, BRP has been localized to the platform of the T-bar ribbon by using advanced optical imaging (Kittel et al., 2006) that relies on the easy visualization of presynaptic boutons. Related studies on other synapses in *Drosophila* are mostly lacking. A previous confocal study reveals several synaptic epitopes in the terminals of the compound eye's photoreceptors (Hiesinger et al., 2001), but such studies rarely attain a resolution sufficient to differentiate the subcellular localizations, and therefore little is known regarding the precise localization of proteins in the T-bar ribbon or associated synaptic organelles.

To address this need, immuno-electron microscopy (immuno-EM) is required. For that purpose, photoreceptor synapses in *Drosophila* are the more convenient, because a single section of the first optic neuropil, or lamina, cuts through an array of modules, or cartridges each containing six photoreceptor terminal profiles, to reveal many synaptic sites (Meinertzhagen, 1996). The profiles are of the six outer photoreceptors, R1–R6 (Meinertzhagen and O'Neil, 1991) and have been extensively used to characterize the ultrastructural phenotypes of synaptic mutants (Stowers et al., 2002; Fabian-Fine et al., 2003).

Even though the molecular mechanisms underlying the assembly and function of T-bar ribbons and other synaptic organelles in *Drosophila* are still not clear, several ribbon-associated proteins have now been identified (Wagh et al., 2006). To gain further insight into the molecular machinery underlying neurotransmitter release at photoreceptor synapses,

as well as to develop a panel of markers with specific patterns of expression at synaptic sites, we studied the localization of candidate protein components of pre-and postsynaptic organelles, using immuno-EM with the pre-embedding method. We concentrated on antibodies that labeled either the T-bar ribbon itself, or that displayed a complementary pattern of labeling. Our ultimate objective was to identify at least one antibody marker for each class of synaptic organelle, and in this report we present final data on a panel of eight such antibodies.

MATERIALS AND METHODS

Animals

Adult wild-type *Drosophila melanogaster* (Oregon R) were used for immunolabeling experiments; two lines, *Drosophila* GAL4 line *Eaat1* -GAL4 and a UAS line UAS-*mCD8::gfp* (on X) (Bloomington Stock Center, Bloomington, IN), were used to generate green fluorescent protein (GFP) expression in lamina T1 cells. Flies were kept under a 12:12-hour light/dark cycle at 24°C and were mostly sacrificed during Zeitgeber time (ZT) 1 to ZT5.

Antibody immunogen and specificity information

We used the following primary antibodies (Table 1), obtained from the sources listed, with tests of specificity on *Drosophila* tissue as given below.

Three mouse monoclonal antibodies arose in a hybridoma screen against a *Drosophila* head homogenate (Hofbauer, 1991), as follows:

1. nc82, which recognizes *Drosophila* BRP (Kittel et al., 2006), was obtained from Dr. E. Buchner (Lehrstuhl für Genetik und Neurobiologie, Biozentrum, Würzburg, Germany) or from DSHB (Iowa City, IA). The specificity of nc82 against BRP protein has been demonstrated in three ways: from the expression pattern of GFP-tagged *bruchpilot* driven under tissue-specific drivers, which completely matches nc82 signals in wing discs and tracheal cells, and also in the active zone of larval NMJ buttons (Wagh et al., 2006); from Western blots of adult head extracts using nc82, in which the antibody recognizes two proteins of about 190 and 170 kDa apparent size (Wagh et al., 2006); and because immunoexpression is lost in *brp* mutant NMJs and rescued by expressing BRP at NMJs in *brp* mutants (Kittel et al., 2006). This antibody has been widely used to label synaptic sites in *Drosophila* , based largely on the pattern of labeling demonstrated at NMJs, but its specificity is in fact mostly not complete for synapses of the CNS outside the NMJ.
2. aa2/2, also from Dr. E. Buchner, is specific for an epitope of the EPS-15 protein, a *Drosophila* homologue of epidermal growth factor receptor pathway substrate clone 15, as revealed by the loss of immunoreactivity in a mutant for the *Eps-15* gene (Hofbauer et al., 2009).
3. Anti-CSP (anti-DCSP-1 or ab49; Zinsmaier et al., 1990), obtained from Dr. K.E. Zinsmaier (Division of Neurobiology, Arizona Research Laboratories, Tucson,

AZ), is widely used as a synaptic protein marker. Its specificity has been confirmed by both Western blots of wild-type head homogenate, in which the antibody recognizes at least four different CSP isoforms at 32, 33, 34, and 36 kDa and the lack of immunolabel in a *csp* null mutant (csp^{U1}) (Eberle et al., 1998).

Three other mouse monoclonal antibodies derived from different sources were also used, as follows:

4. SUK4, from DSHB, was raised against the 130-kDa heavy chain of sea urchin egg kinesin, and Western blotting has shown that it cross-reacts with *Drosophila* embryo 116-kDa heavy chain kinesins (Ingold et al., 1988), as well as the heavy chain of kinesins isolated from bovine brain and sea urchin egg (Ingold et al., 1988).

5. Anti-Discs large (DLG; antibody 4F3 from DSHB), was raised against an *Sma* I-*Eco* RV fragment that includes the second PDZ domain of DLG fused to GST (Dr. Daniel Woods, personal communication; for the exact coding region see Supplemental Fig. S1). It labels larval NMJs in a pattern (Parnas et al., 2001) that is similar to that of a polyclonal anti-DLG widely used to label the *Drosophila* larval NMJ; mutant *dlg* larvae exhibit altered expression of the latter and striking changes in NMJ structure (Lahey et al., 1994).

6. Anti-synapsin (SYNORF1 or antibody 3C11), obtained from either Dr. E. Buchner or DSHB, was raised against a 66-kDa 3′-fusion protein comprising a synapsin protein 5′ fragment corresponding to the nucleotide sequence 621–1967 given in Figure 1 of Klagges et al. (1996) fused to GST; it recognizes four or five synapsin isoforms in Western blots of fly head homogenates (Klagges et al., 1996). The specificity has been confirmed by both Western blot and immunohistochemistry by using a null mutant, syn^{79} , in which the expression of none of the wild-type synapsin isoforms at 70–80 kDa and 143 kDa is seen (Godenschwege et al., 2004).

Finally, two rabbit polyclonal antibodies were used, as follows:

7. Anti- *Drosophila* p21 activated kinase (DPAK) was provided by Dr. N. Harden (Institute of Molecular Biology and Biochemistry, Simon Fraser University, Vancouver, BC, Canada). It was raised against an N-terminal DPAK-GST fusion protein containing the first 166 amino acids of DPAK (Dr. Nicholas Harden, personal communication). The affinity-purified anti-DPAK detects a single band of about 75 kDa in Western blots of extracts prepared from *Drosophila* embryos, which is almost consistent with the predicted molecular mass of 76 kDa for DPAK (Harden et al., 1996).

8. An antibody against Dynamin (2074) was provided by Dr. Mani Ramaswami (University of Arizona, Tucson, AZ). It was raised against a 66-kDa fragment of *Drosophila* Dynamin, lacking the N-terminal 241 amino acids (lacking the GTP-binding domain), fused to the maltose-binding protein (MBP) (Estes et al., 1996). In Western blots against proteins from fly head lysates, the antibody

labels a ~ 92–94-kDa doublet, the appropriate size for the *Drosophila* Dynamin (Gass et al., 1995).

In addition to the eight primary antibodies listed above, a mouse monoclonal antibody against GFP (antibody 3E6, cat. no. A11120, Molecular Probes, Eugene, OR) was used at a dilution of 1:200 for the purpose of enhancing GFP signals driven under the regulation of an *Eaat1* -GAL4 driver. This antibody gives no signal in wild-type *Drosophila* (Johard et al., 2008) and is thus specific to the GFP transgene.

Immunofluorescence confocal microscopy

Fly heads were fixed with 4% paraformaldehyde (PFA) in 0.067 M phosphate buffer (PB; pH 7.4) except for anti-CSP and SUK4 immunolabeling, in which case heads were fixed with either a mixture of 3.75% acrolein and 2% PFA (anti- CSP), or 4% acrolein alone (SUK4). After washing in 0.01 M phosphate-buffered saline (PBS; pH 7.3), the heads were embedded in agarose and sliced at 80-μm thickness. Slices were incubated with 1% sodium borohydride in PBS for 20 minutes at 22°C, to remove eye pigment, then in PBS containing 0.5% Triton X-100 (PBST) with 10% normal goat serum (NGS) for 1 hour at 22°C, and finally in a primary antibody from the list in Table 1, for 2 days at 4°C.

After washing in PBST, slices were blocked in PBST with 10% NGS for 1 hour at 22°C, and subsequently incubated overnight at 4°C in a secondary antibody (1:200). As a secondary antibody, goat anti-mouse or -rabbit IgG conjugated to Cy3 (Jackson ImmunoResearch, West Grove, PA), and goat anti-mouse or -rabbit IgG conjugated to Alexa Fluor 488 (Molecular Probes) were used. Primary and secondary antibodies were diluted in PBST containing 10% NGS. After washing in PBST and PBS, sections were mounted in Vectashield (H-1000; Vector, Burlingame, CA) beneath # 0 coverglasses (VWR, West Chester, PA).

Immunolabeled slices were imaged by using either a Zeiss LSM 410 confocal microscope (Carl Zeiss, Jena, Germany) equipped with Plan Neofluar 40×/1.3 and 100×/ 1.3 oil immersion objectives or, mostly, a Zeiss LSM 510 confocal microscope equipped with Plan Neofluar 40×/ 1.3 and Plan Apochromat 100×/1.4 oil immersion objectives. Alexa 488 excited with an argon laser at 488 nm was viewed through a 515–565-nm band-pass filter, and Cy3 excited with a HeNe laser at 548 nm through a 560-nm long-pass filter. Confocal slices were acquired at a size of 1,024 ×1,024 pixels.

Pre-embedding immuno-electron microscopy

The heads of adult flies were fixed in a mixture of 3.75% acrolein and 2% PFA in 0.067 M PB. After washing in PBS, the heads were embedded in Agarose and sliced at 80-μm thickness. Slices were incubated with 1% sodium borohydride in PBS for 20 minutes at 22°C, then in PBS with 0.07% Triton X-100 (PBST) containing 1% bovine serum albumin (BSA) and 10% NGS for 1 hour at 22°C, and finally in a primary antibody from the list in Table 1, for 2 days at 4°C. After washing in PBST, slices were blocked in PBST containing 1% BSA and 10% NGS for 1 hour at 22°C, and subsequently incubated overnight at 4°C in a 1:100 secondary anti-mouse or anti-rabbit IgG conjugated to 1.4-nm gold (Nanoprobes, Yaphank, NY). Primary and secondary antibodies were diluted in PBST containing 1% BSA

and 10% NGS. After washing in PBST and PBS, slices were fixed in 2% glutaraldehyde in PBS for 10 minutes at 22°C. After fixation, tissues were washed in PBS and distilled water, incubated in a silver enhancement solution (IntenSE™ M Silver Enhancement Kit, cat. no. RPN491; Amersham Biosciences, Bucks, UK), briefly washed in distilled water and PBS, and postfixed with 0.5% osmium. After dehydration, sections were embedded in Poly/Bed 812 resin (Poly-sciences, Warrington, PA). Ultrathin sections were contrasted with uranyl acetate and lead citrate for 30 seconds each. Preparations were examined at 80 kV by using a Tecnai 12 electron microscope (FEI, Hillsboro, OR), and images were captured by using a Kodak Megaview II digital camera and software (AnalySIS, SIS, Münster, Germany).

Image processing and statistical analysis of immuno-EM micrographs

The size, contrast, and brightness of the images were adjusted by using Photoshop 6.0 (Adobe Systems, Tokyo, Japan) and Corel Draw 9.0 (Corel, Ottawa, ON, Canada). For statistical examination of immunogold particles, profile areas were measured by using software (Image J, NIH). To determine the density of silver-enhanced immunogold particles, we counted particles that lay over an area containing profiles of the organelles of interest and by a 20-nm corridor surrounding the profiles. This corridor allowed for inaccuracies between the locations of the epitope and immunogold particle that arise from the maximum combined extension of a complex comprising the primary and secondary immunoglobulin molecule surmounted by a 5-nm gold particle (9+9+2.5=20.5 nm: Griffiths, 1993). For aa2/2 labeling, the number of enhanced gold particles was counted from nine cartridges. For anti-DLG labeling, counts were undertaken by using five images, each of about 200 μm^2 and containing seven or eight cartridge profiles. A Student's t-test was used for tests of statistical significance.

RESULTS

Our analysis is based on the geometrically regular, modular organization of the visual system in wild-type *Drosophila* , which originates in the pattern of innervation from the photoreceptors of the retina. These project axons to the two outermost optic neuropils, the lamina and medulla (Fig. 1A). In the lamina, synaptic input from R1–R6 is provided at approximately 50 release sites per R1–R6 terminal, at so-called tetrad synapses (Meinertzhagen and O'Neil, 1991; Meinertzhagen and Sorra, 2001). Two of the four postsynaptic elements at each tetrad are paired spines of lamina cells L1 and L2, with the other two being contributions from other lamina cells, to form a common postsynaptic cluster (Fig. 1B–D). An individual cartridge comprises the six R1–R6 photoreceptor terminals and the fixed constituency of lamina neurons these innervate, including L1 and L2 (Fig. 1C). The entire group is in turn surrounded by three epithelial glial cells (Fig. 1E) (Meinertzhagen and O'Neil, 1991), which invaginate the terminals at capitate projections (Fig. 1F) (Stark and Carlson, 1986), specialized organelles that are sites of vesicle membrane endocytosis (Fabian-Fine et al., 2003). At the presynaptic active zone of each tetrad, a T-bar ribbon comprises a pedestal surmounted by a platform decorated with synaptic vesicles (Fig. 1G).

To examine the expression pattern of synaptic proteins at *Drosophila* photoreceptor synapses, we first used confocal microscopy to validate candidate antibodies that recognize

the lamina neuropil, and then used immuno-EM to examine the subcellular location of each respective antigen. For all antibodies we used the pre-embedding method. This required that we develop new protocols that could preserve ultrastructure without significant loss of the immunosignal. The organelles of the lamina terminals of fly R1–R6 photoreceptors exhibit various daily and circadian rhythms (Pyza and Meinertzhagen, 1997) and, insofar as protein expression may underlie such changes, we examined flies only in the first part of their day (ZT1–ZT5), both to avoid possible variations in protein expression levels and because our primary aim was to characterize the subcellular locations of synaptic proteins rather than their temporal or functional variations.

Immunofluorescence

A number of candidate antibodies (aa2/2 [anti-ESP-15], nc82 [anti-BRP], SUK4 [anti-kinesin], and those against DLG, DPAK, Dynamin, Fasciclin II, Synapsin, Neural Synaptobrevin, and Syntaxin) have been examined to identify those that immunolabel the lamina neuropil (Hiesinger et al., 2001; the present study). Some of these (against CSP, DLG, neuronal Synaptobrevin, and Syntaxin) have been previously identified by light microscopy (Hiesinger et al., 2001; Kolodziejczyk et al., 2008). In the final selection, we used the eight antibodies listed in Table 1. All labeled the lamina neuropil as well as the medulla and neuropils in the brain. At high magnification, the lamina sites labeled by each antibody differed, however, even though confocal imaging could not reveal the precise subcellular location.

Single immunolabeling

Antibody nc82 (Hofbauer, 1991; Hofbauer et al., 2009) recognizes BRP, a *Drosophila* homologue of vertebrate ELKS/CAST, a component of the vertebrate active zone (Kittel et al., 2006). Anti-BRP has been widely used as a presynaptic marker, especially at the larval NMJ (Budnik and Ruiz-Canada, 2007), but a more general pattern of immunoreactivity in certain regions of the *Drosophila* brain has also been reported (Wagh et al., 2006). Confirming a previous report (Wagh et al., 2006), it strongly labeled the lamina neuropil as well as neuropils in the medulla and central brain (Fig. 2A), revealing that BRP immunoreactivity broadly expresses throughout the *Drosophila* CNS. In lamina cross sections, the signals appeared to be largely restricted to the ring of R1–R6 terminals within the cartridge, which contain most presynaptic sites (Meinertzhagen and Sorra, 2001) and where nc82 signal showed a punctate distribution (Fig. 2B). The counts of BRP-positive puncta given below suggest numerically that most synaptic sites in the lamina are BRP immunopositive.

Antibody aa2/2 recognizes a protein that co-localizes with dynamin to the peri-active zone at NMJs (Hofbauer et al., 2009). The antigen has recently been identified as a *Drosophila* homologue of EPS-15 (Hofbauer et al., 2009). Anti-EPS-15 labeled the neuropil region of the lamina clearly, as well as the medulla and central brain neuropils (Fig. 2C). Staining intensity was uniformly high among the different neuropils, suggesting abundant expression of EPS-15 through the *Drosophila* CNS. In cross sections of the lamina, aa2/2 labeling revealed the outlines of R1–R6 terminals. Particularly strong signals were seen at sites

facing the interior of the cartridge, where many tetrad pre-synaptic sites and their postsynaptic L-cell spines lie (Fig. 2D).

CSP is a presynaptic protein with homology to vertebrate synaptic proteins (Zinsmaier et al., 1990) that seems to increase the Ca^{2+} sensitivity of vesicle exocytosis (Dawson-Scully et al., 2000). It is tightly associated with membranes of synaptic vesicles, and genetic studies in *Drosophila* and mice indicate that CSP is critical for regulated neurotransmitter release (Zinsmaier et al., 1994). Anti-CSP antibody was previously shown to label neuropil regions of the fly's brain (Zinsmaier et al., 1990), and to exhibit a rather diffuse signal in R1–R6 terminals in the lamina (Hiesinger et al., 2001). In addition to the lamina, strong anti-CSP signals were also detected in the medulla and central brain neuropils (Fig. 3A), implying the abundant expression of CSP in different neuropils, as for BRP and EPS-15. As for EPS-15, CSP immunosignal was broadly seen in the R1–R6 terminals, but appeared especially to line the borders facing the cartridge interior, where the tetrads are most concentrated (Fig. 3B).

Antibody SUK4 is a mouse monoclonal antibody raised against the 130-kDa heavy chain of sea urchin egg kinesin (Ingold et al., 1988). Anti-kinesin heavy chain labeled the lamina neuropil (Fig. 3C), but the signal was both weak and diffuse. In contrast to anti-BRP labeling, however, neuropils in the medulla and central brain were hardly labeled. In cross-sectioned lamina cartridges, not only the profiles of R1–R6 terminals but also the surrounding epithelial glia were labeled, leaving two profiles lacking in immunoreactivity, probably those of the L1 and L2 axons at the cartridge axis (Fig. 3D).

The *Drosophila* tumor suppressor gene *discs-large* (*dlg*) is a member of the vertebrate membrane-associated guanylate kinase (MAGUK) family (Woods and Bryant, 1993) that contains the postsynaptic density protein (PSD)-95 (Thomas et al., 1997). Anti-DLG labels synapses and has been widely used as a synaptic marker at the *Drosophila* larval NMJ, where it labels both pre- and postsynaptic sites (Lahey et al., 1994; Chen and Featherstone, 2005). It is also reported to label the lamina (Kolodziejczyk et al., 2008). In our preparations, it labeled the lamina strongly compared with the medulla and central brain regions (Fig. 3E), suggesting abundant expression of DLG in the lamina. Lamina cross sections exhibited a bright ring of R1–R6 terminals after immunolabeling with anti-DLG; the signals were sharply localized to regions of the photoreceptor membrane, which sometimes appeared to have an immunoreactive substructure (Fig. 3F). By contrast, the interior of R1–R6 terminal profiles had little label.

DPAK is a *Drosophila* homologue of the serine/ threonine kinase PAK, a target of the Rho subfamily proteins Rac and Cdc42 (Harden et al., 1996; Mentzel and Raabe, 2005) that are important regulators of the actin cytoskeleton (Bagrodia and Cerione, 1999). DPAK localizes most obviously to the postsynaptic side of presynaptic varicosities at *Drosophila* NMJs (Sone et al., 2000; Rohr-bough et al., 2007). In the optic lobe, anti-DPAK antibody mainly labeled the lamina neuropil, compared with which the signals in the medulla and central brain were rather weak (Fig. 4A). In lamina cross sections the anti-DPAK signal showed a punctate distribution (Fig. 4B). This was rather like the pattern for nc82 (anti-BRP) labeling, relative to which DPAK immunolabeled puncta did not reveal the cartridge

structure clearly, and appeared to be larger and fewer, and to originate in components other than R1–R6, however (Fig. 4B).

Finally, we examined an antibody against *Drosophila* synapsin (SYNORF1) (Klagges et al., 1996). Synapsins are a small family of synaptic vesicle-associated phosphoproteins that participate in regulating neurotransmitter release (Südhof et al., 1989), although their exact function is still controversial. SYNORF1, anti-synapsin, detects an epitope that is widely conserved in arthropod nervous systems, and labels not only synapses in insects but also those in crustaceans (Harzsch et al., 1999) and spiders (Fabian-Fine et al., 1999). In *Drosophila* , anti-synapsin labeled the lamina as well as medulla and central brain neuropils. Unlike other antibodies we used, however, immunosignals in the medulla and central brain were stronger than those in the lamina (Fig. 4C), suggesting that *Drosophila* synapsin is much more abundant in the medulla and brain. In lamina cross sections the signal was spread diffusely in the ring of R1–R6 terminals but also showed a distribution of clustered puncta and, like anti-DPAK immunolabeling, failed to reveal clear geometrical cartridge structures (Fig. 4D).

Expression of *Eaat1* -GAL4 in lamina T1 cells

We examined *Eaat1* -GAL4 driver expression by means of the GAL4/UAS system, by using UAS- *mCD8::gfp* as an effector line. To enhance the expression of GFP signals we immunolabeled preparations with anti-GFP, subsequently detected by a secondary antibody conjugated to Alexa Fluor 488, before examination by confocal microscopy. The signal strength was otherwise too low to reveal the entire projection pattern of individual cells. In horizontal slices of the optic lobes of *Eaat1>mCD8::gfp* flies, a population of neurons with cell bodies lying in the anterior and posterior regions of the medulla cortex was labeled with anti-GFP. These cells had axons extending across the outer chiasm before penetrating the lamina neuropil, where they formed the basket-like terminals (Fig. 5) that are typical of T1 cells (Fischbach and Dittrich, 1989). GFP signals were also visible in some fibers innervating the medulla neuropil as well as some cell bodies overlying the medulla, beneath the lamina neuropil (Fig. 5). In lamina cross sections, GFP expression revealed six to seven tiny profiles of the basket-like ending (cf. Fig. 6D) with a distribution fully compatible with the β -processes of T1 cells identified by serial-EM (Meinertzhagen and O'Neil, 1991). According to the morphological properties described above, we assigned the *Eaat1* -GAL4-driven GFP-expressing medulla cells to T1 cells, and their lamina terminals to T1's basket endings.

Double immunolabeling

The opportunities for double labeling with different combinations of the eight antibodies were restricted, because most successful signals were generated by mouse monoclonal antibodies. Double labeling with anti-BRP (nc82) and anti-DPAK was first performed, however, to study the relative distributions of these two epitopes in the terminals of R1–R6, because both antibodies are directed against synaptic proteins that had previously been identified at the larval NMJ, and because their immunosignals showed similar distribution patterns to each other in the lamina neuropil. With both antibodies, the signals of nc82, a widely used presynaptic marker, lay close to those of anti-DPAK, but neither exactly

opposite nor overlapping the latter, therefore suggesting that DPAK originates in different organelles from those that express BRP (Fig. 6A–C). Subsequently, the subcellular distribution of DPAK was characterized by examining *Eaat1>mCD8::gfp* flies. After double immunolabeling the lamina terminals of R1–R6 in *Eaat1>mCD8::gfp* flies with both anti-DPAK and anti-GFP, we found that the anti-DPAK signals localized to sites that lay opposite and partly overlapped the distal tip of each T1 cell basket ending profile (Fig. 6D–F).

Double-immunolabeling with anti-Dynamin, and either aa2/2 (anti-EPS-15) or anti-DLG, was also performed to gain insight into their relative distributions. In lamina cross sections, Dynamin and EPS-15 almost completely co-localized to the cytoplasm of the R1–R6 terminals (Fig. 6G–I). Dynamin is required for scission of newly endocytosed vesicles from the plasma membrane (reviewed in Hinshaw, 2000). EPS-15 is considered to localize, together with Dynamin, to the cytoplasm around the site for vesicle endocytosis, which in R1–R6 terminals is the capitate projections (Fabian-Fine et al., 2003). In contrast, anti-Dynamin and anti-DLG signals displayed a complementary pattern of distribution, both being closely associated in R1–R6 terminals, but hardly overlapping within these. Dynamin signals appeared to surround those of DLG (Fig. 6J–L).

To resolve these antigen expression sites more closely, we next developed immuno-EM protocols for each antibody.

Immunoelectron microscopy

Of the eight antibodies that gave a clear pattern of labeling in the lamina terminals of R1–R6, five— anti-BRP (nc82), anti-EPS-15 (aa2/2), anti-CSP, anti-kinesin (SUK4), and anti-DLG— successfully labeled particular structures in these terminals at the EM level. Anti-Dynamin was not tested by EM because its distribution was too widespread, whereas the other two antibodies, antisynapsin and anti-DPAK, failed to show clear labeling at the EM level. The most obvious reason for the reduced signal seen after immuno-EM with any antibody is that the thinner sections include far less epitope than thicker slices viewed for light microscopy. However, other factors— the different fixatives used for EM preparation, which may denature some epitopes but not others, or the loss of immunosignal during the lengthy procedure required to prepare EM specimens— affect the use of particular antibodies. These seem to have been critical for anti-synapsin and anti-DPAK, both of which gave a clear lamina immunofluorescence signal. In this study, for immuno-EM we tried neither PFA alone, glutaraldehyde alone, nor a combined fixative of PFA and glutaraldehyde. Even if not optimal for epitope preservation, fixation with acrolein gave well-preserved tissue that was essential to see clear organelle substructure. The choice of different fixatives may improve preservation of the epitopes for anti-synapsin and DPAK, and may prove successful in future trials.

Two antibodies, nc82 (anti-BRP) and SUK4 (anti-kinesin), gave immunosignals that localized to different regions of the T-bar ribbon at photoreceptor tetrads.

First, anti-BRP signals at tetrad synapses were detected at the edge of the ribbon’s platform, usually to one side only, but never to the pedestal (Fig. 7A–C). Their presence at this site

confirms at higher resolution a previous report using subdiffraction resolution stimulated emission depletion (STED) fluorescence microscopy at the NMJ, where anti-BRP also labels a similar domain around the platform edges of T-bar ribbons (Kittel et al., 2006). For the synaptic terminals of R1–R6, our immuno-EM findings help to clarify the loss of platforms from T-bar ribbons seen at the photoreceptor tetrads of flies in which *brp* is suppressed by *brp* -RNAi (Wagh et al., 2006).

In contrast to anti-BRP immunolabeling, anti-kinesin (SUK4) (Fig. 7D,E) immunosignals appeared beneath the platform of the T-bar ribbon, localized to the sides of its pedestal. Two antibodies labeled the synaptic vesicles that surround the T-bar ribbons of the tetrad synapses. First, the signal recognized by anti-EPS-15 (aa2/2) antibody appeared among the vesicle pool in the cytoplasm of photoreceptor terminals, and often close to the capitate projection (Fig. 8A–C). Most immunogold particles were at a distance that exceeded 20 nm from the capitate projection profile, however, indicating that aa2/2 does not recognize the actual capitate projection but rather some epitope nearby. Capitate projections are sites of clathrin-mediated endocytosis in R1–R6 terminals (Fabian-Fine et al., 2003), and thus the origin of the vesicle cycle, suggesting that the anti-EPS-15 epitope lay close to the origin of newly endocytosed vesicle membrane.

Synaptic vesicles are small (about 30 nm in diameter), densely packed (about 800 vesicles per μm^3: Borycz et al., 2005; with a spacing between vesicle profiles of about 65 nm: Fabian-Fine et al., 2003), and poorly preserved by the pre-embedding procedures we used, however. We were therefore not able to localize the anti-EPS-15 epitope directly to the vesicle membrane. Instead, we calculated the immunogold signal density and found that the density of gold particles in the profiles of R1–R6 (0.97 ± 0.36 [mean ± SD] per μm^2) was higher than that in monopolar cells (0.16 ± 0.33 per μm^2). The profile area of the lamina cartridge cross section is mostly occupied by the profiles of R1–R6 terminals and the axon profiles of the monopolar cells, and confocal images have demonstrated that EPS-15 is strongly expressed in R1–R6, but not in the monopolar cells (Fig. 2D). For this reason, we chose the monopolar cell profiles to compare against the R1–R6 signal density. Furthermore, within photoreceptor terminals, most signal was located over the synaptic vesicle pool (1.15 ± 0.35 per μm^2), more than three times higher than that over the photoreceptor membrane (0.34 ± 0.55 per μm^2). Both differences were significant ($P < 0.01$; t-test). Thus the anti-EPS-15 antigen is concentrated over and appears to localize to the vesicle pool in the synaptic terminals of R1–R6.

Anti-CSP signal was detected in the cytoplasm of R1–R6 terminals very close to the electron-dense T-bar ribbon surrounded by synaptic vesicles (Fig. 8D–F). CSP is a vesicle-associated protein and also a potential link protein between presynaptic calcium channels and synaptic vesicles (Mastrogiacomo et al., 1994). It is therefore not unexpected that anti-CSP signals are located at the presynaptic active zone decorated by synaptic vesicles.

Anti-DLG signals were detected almost exclusively in the R1–R6 photoreceptor terminals (Fig. 9A). Within the terminals, immunoreactivity was often seen close to the heads of capitate projections, but not the stalks (Fig. 9B–E). Capitate projections are invaginations from surrounding epithelial glia and specialized organelles for the endocytosis of vesicle

membrane, and possibly histamine recycling (Fabian-Fine et al., 2003). They are thus sites to produce newly endocytosed synaptic vesicles, and often lie close to the presynaptic T-bar ribbon. Localization of immunogold particles to the heads of capitate projections was confirmed by calculating the signal density of DLG immunoreactivity. The density at the heads was 1.38 ± 0.45 per μm^2, whereas that in other regions of the lamina was 0.15 ± 0.03 per μm^2. The difference was significant ($P < 0.01$; t-test). Furthermore, immunogold particles were always located on the photoreceptor side of capitate projection head profiles, not over the head itself. Thus the epitope appears to be associated with the photoreceptor membrane facing the capitate projection heads, rather than with the invaginating glial cell at their center.

Quantitative features of antibody labeling

Even with the limited panel of antibodies that gave good immunosignals in the lamina, our immuno-EM data clearly revealed the synaptic locations of several epitopes. The signals fail, however, to identify whether all synapses express the protein epitope or only a subset of these. This is because the signal seen after immuno-EM is usually weak, and we may therefore expect to label only some of the synapses that actually express the protein. Thus even in the most favorable preparations using the nc82 antibody, only about 10% of tetrad ribbons actually exhibited labeling at the EM level. This low frequency explains why tetrad sites were generally never seen at which both sides of a platform of the T-bar ribbon were labeled, even though this is predicted statistically from the combined probabilities of epitope labeling for each side. A 10% probability of unilateral labeling would be less than a 1% probability of a bilateral one, which is too few to detect reliably. The doubly labeled pedestals seen with SUK4 (Fig. 7E) indicate that the T-bar ribbon is nevertheless symmetrical.

Based on knowledge of the subcellular distribution of the epitopes gained from our immuno-EM, it was possible to count the numbers of immunopuncta seen with confocal microscopy, and compare these with the numbers of synaptic sites previously reported from conventional EM (Meinertzhagen and Sorra, 2001). This comparison was undertaken for anti-BRP (nc82) immunolabeling, and enabled us to establish whether all synaptic sites expressed BRP, or only a small subset, possibly only the tetrads. Our EM observations indicated that only tetrad T-bar ribbons were immunolabeled, but not other types of synapse, which are also relatively numerous (Meinertzhagen and Sorra, 2001). Counts of BRP immunopuncta seen in confocal serial sections of nc82-immunolabeled lamina revealed an average of 13.7 ± 1.5 per micron depth (mean± SD of the means from three 14-μm image stacks, each derived from a different cartridge). All puncta were counted, including ones that were weakly labeled. In contrast, a total of 480 synapses, 283 of them being tetrads, were reported from serial-EM of an entire single wild-type cartridge (Meinertzhagen and O'Neil, 1991; Meinertzhagen and Sorra, 2001). These were distributed through 366 60-nm-thick sections, and thus through a depth of 22 μm. Even though the distribution of sites is not uniform (Hauser-Holschuh, 1975; Meinertzhagen and Sorra, 2001) and section thickness not reliably calibrated, this would lead to a prediction of 21.9 synapses per micron depth in a single lamina cartridge, 12.9 of which are tetrads. The predicted number of tetrads per micron

depth roughly matches that of BRP-positive fluorescent puncta (13.7) calculated from our confocal data.

These numerical considerations thus suggest that the BRP immunopuncta could identify all tetrad sites, or alternatively ~ 60% of synaptic sites in the lamina overall, including both tetrads and non-tetrads. Random searches through many lamina cartridges in our immuno-EM preparations revealed nc82-positive T-bar ribbons at tetrad synapses only, however. This suggests that immunoreactivity to BRP was not present at non-tetrad synapses, either because the ribbons at these sites contained too little protein to detect, or because they lack BRP entirely. Given the structural uniformity of T-bar ribbons at different classes of lamina synapse (Meinertzhagen and O'Neil, 1991), the latter possibility seems to us unlikely.

DISCUSSION

This study was conducted to gain further insight into the molecular machinery underlying neurotransmitter release at *Drosophila* photoreceptor synapses, as well as to develop a panel of markers to recognize synaptic sites and organelles involved in neurotransmitter release. For this, we used antibodies against a number of proteins, chosen principally for their favorable expression patterns as components of pre- and/or postsynaptic sites, and screened from among a larger set of antibodies, by means of confocal microscopy. Our findings extend those of two previous reports in particular, on expression of synaptic proteins in the lamina (Hiesinger et al., 2001) and neurotransmitter phenotypic markers (Kolodziejczyk et al., 2008). All the antibodies listed in Table 1 immunolabeled R1–R6 photo-receptor terminals in the lamina, often (kinesin, DLG, and DPAK antibodies) more strongly than neuropils of the medulla or central brain, but sometimes (anti-synapsin) more weakly.

The subcellular localizations of these antibody signals clearly differed. Even at the level of light microscopy, some antibody signals were clearly punctate, compatible with the labeling of synaptic sites and other focally distributed organelles. However, only immuno-EM observations enabled us to distinguish clearly the subcellular localization of each antigen relative to others, in locations summarized in Figure 10.

BRP and kinesin antibodies recognize different sites at the T-bar ribbon

Our findings show that antibody nc82 recognizes a restricted region at the edge of the platform of the T-bar ribbon of photoreceptor tetrad synapses in the lamina. Its antigen, BRP, a *Drosophila* homologue of the mammalian CAZ protein, CAST (Wagh et al., 2006), is a 200-kDa coiled-coil protein. Mutant study suggested that BRP is a structural protein of the platform of *Drosophila* T-bar ribbon because the platform is missing in *brp* mutants (Wagh et al., 2006), consistent with our immuno-EM findings. Until now, however, even though the subcellular localization of BRP at presynaptic active zones has been proposed from confocal microscopy, the precise location has been elusive because of the resolution limitation of light microscopy. A single report using STED fluorescence microscopy has shown doughnut-shaped profiles of nc82 immunolabeling centered at active zones of *Drosophila* neuromuscular synapses (Kittel et al., 2006). Synapses elsewhere, in the central brain or visual system, have not been examined in such detail, but our finding that the nc82 antigen (BRP) is clearly located at the edge of the T-bar ribbon platform at the tetrad

synapses of R1–R6 is consistent with these data from NMJs, and suggests that BRP may also be a constituent of the platform of T-bar ribbons at lamina synapses in *Drosophila* , at least those at tetrad synapses, whereas the expression of BRP more generally in the brain indicates that such expression sites must be widespread, possibly at most synapses.

An epitope at the side of the pedestal of the T-bar ribbon was recognized by SUK4, a monoclonal antibody that cross-reacts with *Drosophila* heavy chain kinesins (Ingold et al., 1988). Although both BRP and kinesin heavy chain are clearly localized to the T-bar ribbon at the EM level, the distribution patterns of these two proteins appear different in confocal images, in which BRP signals are punctate and kinesin rather more diffuse. Kinesins are a large family of microtubule ATPase motor proteins that direct the movement of intracellular cargoes along microtubules to various destinations within neurons. Such widespread expression of kinesins along the axons might be responsible for the diffuse pattern of immunolabeling with SUK4 compared with the more localized BRP. In a possible counterpart at mouse photoreceptors, immunoreactivity to a kinesin heterodimer, KIF3A, is enriched at the presynaptic ribbon (Muresan et al., 1999; tom Dieck et al., 2005), although its function there is not known. It is possible that at both these non-microtubule sites kinesin helps to convey primed vesicles to the docking/release site at the base of presynaptic ribbons. An alternative view proposes, however, that synaptic ribbons in vertebrate photoreceptors serve to tether vesicles stably in mutual contact via kinesin, so that they can fuse with each other during multivesicular release (Parsons and Sterling, 2003). So far, however, evidence for such a mode of release at *Drosophila* synapses is not available.

The bipartite composition of the tetrad T-bar ribbon

A clear structural subdivision of the T-bar ribbon at photoreceptor tetrads, as well as at other fly synapses, into a platform and pedestal (Burkhardt and Braitenberg, 1976; Fröhlich and Meinertzhagen, 1982), has long been recognized. The specialization of the ribbon platform arose during the course of dipteran evolution, from an ancestral form in which only the structural counterpart of the pedestal is visible (Shaw and Meinertzhagen, 1986), and which resembles the presynaptic ribbon at photoreceptor synapses of other insects, such as the dragonfly (Armett-Kibel et al., 1977). The patterns of expression of two epitopes now reflect a clear separation between pedestal and platform in the synapses of recent flies, with one antibody (against BRP) binding at the platform and the other (against kinesin) at the pedestal.

Presynaptic ribbons at photoreceptor synapses in the vertebrate retina also have a bipartite composition, with separation between the protein components of the ribbon and its underlying arciform density (tom Dieck et al., 2005). CAST, the mammalian homologue of BRP, is localized to a complex containing the arciform density at the base of the ribbon (tom Dieck et al., 2005; Deguchi- Tawarada et al., 2006), along with Bassoon (Brandstätter et al., 1999) and RIM2 (tom Dieck et al., 2005; Deguchi- Tawarada et al., 2006). Piccolo, a second binding partner of CAST, is located in the ribbon. Neither Piccolo nor Bassoon has a *Drosophila* homologue, however. Thus CAST at the ribbon synapse of vertebrate photoreceptors lies next to the presynaptic membrane. BRP in fly photoreceptors, by contrast, despite a postulated role in promoting calcium channel clustering at the presynaptic

membrane (Kittel et al., 2006), is separated from the presynaptic membrane by the height of the pedestal of the T-bar ribbon.

DPAK localizes to sites at the T1 basket cell terminals

Anti-DPAK recognizes the *Drosophila* serine/threonine kinase PAK, which functions in neurons downstream of Dock to regulate axon guidance (Hing et al., 1999; Ang et al., 2003). It also stabilizes the organization of postsynaptic components of the NMJ, and regulates the size of the subsynaptic reticulum (Parnas et al., 2001). Expression of DPAK at *Drosophila* larval NMJs occurs at the postsynaptic membrane (Sone et al., 2000), and is therefore membrane associated, as it is at other sites (Conder et al., 2007). At the NMJ, double-labeling with anti-DPAK and anti-BRP, the latter recognizing the presynaptic T-bar platform, reveals complementary patterns of expression (Wagh et al., 2006). At lamina R1–R6 terminals, by contrast, the same double-labeling did not produce any related pattern of expression between DPAK and BRP, and given our demonstration of BRP localization to the platform of the presynaptic T-bar ribbon, DPAK must therefore not be located at the postsynaptic membrane opposite such sites in the lamina. By contrast, our double-labeling shows that DPAK clearly localizes to sites at or near the distal tips of T1 cell basket terminals. The gnarl junctions, at which an amacrine cell process provides synaptic input to the β -processes of T1, but with a thin insinuating glial sheet between the two elements (Meinertzhagen and O'Neil, 1991), are the most obvious candidates for such sites. This candidacy would suggest that DPAK could express at either pre- or postsynaptic membranes, or possibly both. Resolution of the exact site will depend on successful immuno-EM observation with anti-DPAK.

Anti-DLG signals localize to the heads of capitate projections

DLG is a multifunctional protein, first identified as a tumor suppressor. At the *Drosophila* NMJ, the protein is present at both pre- and postsynaptic sites (Lahey et al., 1994), and is involved in organizing the postsynaptic structure as well as regulating neurotransmitter release (Budnik et al., 1996). At the postsynaptic membrane, DLG serves as a scaffold protein that tethers Fasciclin II and Shaker K^+ channel proteins to the muscle by directly binding to their cytoplasmic tails (Tejedor et al., 1997; Thomas et al., 1997; Zito et al., 1997). In addition to these roles at synapses, DLG protein functions as a critical component of septate junctions and is also required to maintain apicobasal polarity in *Drosophila* epithelia (Woods et al., 1996). Our immuno-EM now reveals that DLG proteins are located on the photoreceptor membrane around the invaginating head of capitate projection organelles. Expression is restricted to the head, rather than the shaft and base, which are the identified sites of vesicle membrane endocytosis (Fabian-Fine et al., 2003). The binding we find in our EM observations, of anti-DLG to the head of the capitate projections, offers an explanation for the complementary signals of anti-DLG and anti-Dynamin seen in double-labeled confocal images, because Dynamin immunosignal is likely to localize to sites for vesicle recovery at the shaft of the capitate projections, closely adjacent to the DLG signal on the overlying head. Although the ultrastructural specialization of the head perhaps qualifies it to play a specific role as a synaptic organelle, for which the recycling of histamine has previously been suggested (Fabian-Fine et al., 2003), its exact function in fact remains unknown. Our findings now suggest that DLG may play a role in tethering proteins,

such as an amine transporter, to the photoreceptor membrane, but confirmation of this will first require identification of specific transporters used in histamine recycling, itself a major challenge (Stuart et al., 2007).

We note that the location of DLG in *Drosophila* photoreceptor terminals bears some similarities to the location of another scaffolding protein, PSD-95, in the mammalian retina. There, PSD-95 is located at presynaptic sites in rod spherule and cone pedicle terminals, as well as in one subset of the dendrites that are postsynaptic to bipolar cell terminals (Koulen et al., 1998).

Localization of CSP and EPS-15 antigen

CSP is a membrane protein that has been evolutionarily conserved in both invertebrate and vertebrate neurons, and is tightly associated with synaptic vesicles, critical for their regulated release of neurotransmitter (Zinsmaier et al., 1994). At *Drosophila* larval NMJs, null *csp* mutants reveal presynaptic defects in the formation of synaptic varicosities and reductions in evoked neurotransmitter release (Dawson-Scully et al., 2007). CSP is also a potential link protein between synaptic vesicles and presynaptic calcium channels, key regulators of neurotransmitter release (Mastrogiacomo et al., 1994), and is required for a late Ca^{2+}-dependent step in vesicle fusion (Nie et al., 1999; Dawson-Scully et al., 2000; Graham and Burgoyne, 2000). These findings suggest that CSP should localize close to the presynaptic active zone, where Ca^{2+} channels encoded by the gene *cacophony* (Kawasaki et al., 2004), that possibly correspond to particles seen from freeze-fractured faces of the presynaptic membranes at both fly larval NMJ (Feeney et al., 1998) and adult tetrad (Fröhlich, 1985) synapses, are arranged to allow efficient vesicle exocytosis. This expectation is fully met by the pattern of subcellular localization revealed by our immuno-EM observations, with immunogold signal found at and around the T-bar ribbon and at the vesicles surrounding it. Thus the location of CSP is fully compatible with the two major functions so far assigned to this synaptic protein, in modulating the Ca^{2+} sensitivity of neurotransmitter release from *Drosophila* NMJs, possibly by regulating presynaptic calcium channels at the active zone (Dawson-Scully et al., 2000); and in mediating a direct step in vesicle exocytosis of adrenal chromaffin cells (Graham and Burgoyne, 2000).

Our data, combined with the loss of vesicles in *csp* mutant R1–R6 photoreceptor terminals (Zinsmaier et al., 1994), suggest that CSP functions at photoreceptor tetrad synapses in a manner similar to that at the larval NMJs of *Drosophila* .

The monoclonal antibody aa2/2 against *Drosophila* EPS-15 labels the periactive zone at *Drosophila* larval NMJs, a region surrounding the active zone that is enriched in proteins involved in endocytosis (Koh et al., 2004; Marie et al., 2004), co-labeling this region with anti-Dynamin (Hofbauer et al., 2009). The same pattern of labeling was also obtained with both antibodies in the lamina terminals of R1–R6. From our observation that Dynamin and EPS-15 both co-localize to the cytoplasm of R1–R6 terminals, in a zone that we might therefore also suspect is endocytotic, and that the patterns of anti-Dynamin and DLG immunolabeling are complementary to this zone, we speculate that EPS-15 expression is located among vesicle pools surrounding the capitate projections. Such subcellular location of EPS-15 has been confirmed by our EM observation. The vesicles surrounding capitate

projections represent those that are recently endocytosed from the capitate projections, and that label with antibodies against Endophilin and Clathrin (Fabian-Fine et al., 2003).

The current study has revealed the differential subcellular localization of five proteins that either are localized to synaptic organelles or are synapse-associated in the lamina terminals of *Drosophila* R1–R6 photoreceptors. These provide an ideal model structure to study synapses in invertebrates. Our results also provided markers for synaptic organelles, and a basis for understanding the synaptic machinery contributing synaptic neurotransmitter release and the vesicle recovery in the photoreceptor terminals. The markers recognizing distinct synaptic organelles will allow investigation of their physiological changes, such as their number and dynamic kinetics, under various physiological conditions using a light microscope in future studies.

Supplementary Material

Refer to Web version on PubMed Central for supplementary material.

Acknowledgments

We thank the following for generous gifts of antibodies and supplying fly strains: Dr. Nicholas Harden (Simon Fraser University, Burnaby, BC, Canada) for anti-DPAK antibody; Dr. Erich Buchner (Biocenter, University of Würzburg, Germany) for anti-BRP, anti-EPS-15, and anti-synapsin; Dr. Konrad E. Zinsmaier for anti-CSP; DSHB for anti- BRP, anti-DLG, anti-synapsin, and SUK4; Dr. Mani Ramaswami for anti-Dynamin; and the Bloomington Stock Center for fly strains. We also thank Mr. Zhiyuan Lu and Ms. Rita Kostyleva for assistance with electron microscopy, and Drs. Nicholas Harden and Daniel Woods for immunogen sequence information for their respective antibodies.

Grant sponsor: National Institutes of Health; Grant number: R01-EY03592; Grant sponsor: Canada Council Killam fellowship (to I.A.M.).

Abbreviations

BRP	Bruchpilot
CNS	central nervous system
CSP	cysteine string protein
DLG	Discs large
DPAK	*Drosophila* p21 activated kinase
DSHB	Developmental Studies Hybridoma Bank
EPS-15	epidermal growth factor receptor pathway substrate clone 15
NMJ	neuromuscular junction

LITERATURE CITED

Akert, K.; Pfenninger, K.; Sandri, C.; Moor, H. Freeze etching and cytochemistry of vesicles and membrane complexes in synapses of the central nervous system. In: Pappas, GD.; Purpura, DP., editors. Structure and function of synapses. New York: Raven Press; 1972. p. 67-86.

Ang LH, Kim J, Stepensky V, Hing H. Dock and Pak regulate olfactory axon pathfinding in *Drosophila*. Development. 2003; 130:1307–1316. [PubMed: 12588847]

Armett-Kibel C, Meinertzhagen IA, Dowling JE. Cellular and synaptic organization in the lamina of the dragon-fly *Sympetrum rubicundulum*. Proc R Soc Lond B. 1977; 196:385–413.

Bagrodia S, Cerione RA. Pak to the future. Trends Cell Biol. 1999; 9:350–355. [PubMed: 10461188]

Borycz JA, Borycz J, Kubów A, Kostyleva R, Meinertzhagen IA. Histamine compartments of the *Drosophila* brain with an estimate of the quantum content at the photoreceptor synapse. J Neurophysiol. 2005; 93:1611–1619. [PubMed: 15738275]

Brandstätter JH, Fletcher EL, Garner CC, Gundelfinger ED, Wässle H. Differential expression of the presynaptic cytomatrix protein bassoon among ribbon synapses in the mammalian retina. Eur J Neurosci. 1999; 11:3683–3693. [PubMed: 10564375]

Brose N, Hofmann K, Hata Y, Südhof TC. Mammalian homologues of *Caenorhabditis elegans unc-13* gene define novel family of C-domain protein. J Biol Chem. 1995; 270:25273–25280. [PubMed: 7559667]

Budnik, V.; Ruiz-Canada, C., editors. International Review of Neurobiology. 2nd ed. Vol. 75. New York: Academic Press; 2007. The fly neuromuscular junction: structure and function.

Budnik V, Koh Y-H, Guan B, Hartmann B, Hough C, Woods D, Gorczyca M. Regulation of synapse structure and function by the *Drosophila* tumor suppressor gene *dlg*. Neuron. 1996; 17:627–640. [PubMed: 8893021]

Burkhardt W, Braitenberg V. Some peculiar synaptic complexes in the first visual ganglion of the fly, *Musca domestica*. Cell Tissue Res. 1976; 173:287–308. [PubMed: 991241]

Burns ME, Augustine GJ. Synaptic structure and function: dynamic organization yields architectural precision. Cell. 1995; 83:187–194. [PubMed: 7585936]

Cases-Langhoff C, Voss B, Garner AM, Appeltauer U, Takei K, Kindler S, Veh RW, De Camilli P, Gundelfinger ED, Garner CC. Piccolo, a novel 420 kDa protein associated with the presynaptic cytomatrix. Eur J Cell Biol. 1996; 69:214–223. [PubMed: 8900486]

Chen K, Featherstone D. Discs-large (DLG) is clustered by presynaptic innervation and regulates postsynaptic glutamate receptor subunit composition in *Drosophila*. BMC Biol. 2005; 3:1. [PubMed: 15638945]

Conder R, Yu H, Zahedi B, Harden N. The serine/threonine kinase dPak is required for polarized assembly of F-actin bundles and apical-basal polarity in the *Drosophila* follicular epithelium. Dev Biol. 2007; 305:470–482. [PubMed: 17383630]

Dawson-Scully K, Bronk P, Atwood HL, Zinsmaier KE. Cysteine-string protein increases the calcium sensitivity of neurotransmitter exocytosis in *Drosophila*. J Neurosci. 2000; 20:6039–6047. [PubMed: 10934253]

Dawson-Scully K, Lin Y, Imad M, Zhang J, Marin L, Horne JA, Meinertzhagen IA, Karunanithi S, Zinsmaier KE, Atwood HL. Morphological and functional effects of altered cysteine string protein at the *Drosophila* larval neuromuscular junction. Synapse. 2007; 61:1–16. [PubMed: 17068777]

De Camilli, P.; Haucke, V.; Takei, K.; Mugnaini, E. Synapses. Cowan, WM.; Südhof, TC.; Stevens, CF., editors. Baltimore, MD: Johns Hopkins University Press; 2001. p. 89-133.

Deguchi-Tawarada M, Inoue E, Takao-Rikitsu E, Inoue M, Kitajima I, Ohtsuka T, Takai Y. Active zone protein CAST is a component of conventional and ribbon synapses in mouse retina. J Comp Neurol. 2006; 495:480–496. [PubMed: 16485285]

Eberle KK, Zinsmaier KE, Buchner S, Gruhn M, Jenni M, Arnold C, Leibold C, Reisch D, Walter N, Hafen E, Hofbauer A, Pflugfelder GO, Buchner E. Wide distribution of the cysteine string proteins in *Drosophila* tissues revealed by targeted mutagenesis. Cell Tissue Res. 1998; 294:203–217. [PubMed: 9799436]

Estes PS, Roos J, van der Bliek A, Kelly RB, Krishnan KS, Ramaswami M. Traffic of dynamin within individual *Drosophila* synaptic boutons relative to compartment-specific markers. J Neurosci. 1996; 16:5443–5456. [PubMed: 8757257]

Fabian-Fine R, Höger U, Seyfarth E-A, Meinertzhagen IA. Peripheral synapses at identified mechanosensory neurons in spiders: three-dimensional reconstruction and GABA immunocytochemistry. J Neurosci. 1999; 19:298–310. [PubMed: 9870959]

Fabian-Fine R, Verstreken P, Hiesinger PR, Horne JA, Kostyleva R, Zhou Y, Bellen HJ, Meinertzhagen IA. Endophilin promotes a late step in endocytosis at glial invaginations in *Drosophila* photoreceptor terminals. J Neurosci. 2003; 23:10732–10744. [PubMed: 14627659]

Feeney CJ, Karunanithi S, Pearce J, Govind CK, Atwood HL. Motor nerve terminals on abdominal muscles in larval flesh flies, *Sarcophaga bullata* : comparisons with *Drosophila*. J Comp Neurol. 1998; 402:197–209. [PubMed: 9845243]

Fischbach K-F, Dittrich APM. The optic lobe of *Drosophila melanogaster* IA Golgi analysis of wild-type structure. Cell Tissue Res. 1989; 258:441–475.

Fröhlich A. Freeze-fracture study of an invertebrate multiple-contact synapse: the fly photoreceptor tetrad. J Comp Neurol. 1985; 241:311–326. [PubMed: 4086659]

Fröhlich A, Meinertzhagen IA. Synaptogenesis in the first optic neuropile of the fly's visual system. J Neurocytol. 1982; 11:159–180. [PubMed: 7062089]

Garner CC, Kindler S, Gundelfinger ED. Molecular determinants of presynaptic active zones. Curr Opin Neurobiol. 2000; 10:321–327. [PubMed: 10851173]

Gass GV, Lin JJ, Scaife R, Wu CF. Two isoforms of *Drosophila* dynamin in wild-type and *shibire* (*ts*) neural tissue: different subcellular localization and association mechanisms. J Neurogenet. 1995; 10:169–191. [PubMed: 8719772]

Godenschwege TA, Reisch D, Diegelmann S, Eberle K, Funk N, Heisenberg M, Hoppe V, Hoppe J, Klagges BRE, Martin JR, et al. Flies lacking all synapsins are unexpectedly healthy but are impaired in complex behaviour. Eur J Neurosci. 2004; 20:611–622. [PubMed: 15255973]

Graham ME, Burgoyne RD. Comparison of cysteine string protein (Csp) and mutant α-SNAP overexpression reveals a role for Csp in late steps of membrane fusion in dense-core granule exocytosis in adrenal chromaffin cells. J Neurosci. 2000; 20:1281–1289. [PubMed: 10662817]

Griffiths, G. Fine structure immunocytochemistry. Heidelberg: Springer-Verlag; 1993.

Gundelfinger ED, tom Dieck S. Molecular organization of excitatory chemical synapses in the mammalian brain. Naturwissenschaften. 2000; 87:513–523. [PubMed: 11198190]

Harden N, Lee J, Loh H-Y, Ong Y-M, Tan I, Leung T, Manser E, Lim L. A *Drosophila* homolog of the Rac- and Cdc42- activated serine/threonine kinase PAK is a potential focal adhesion and focal complex protein that colocalizes with dynamic actin structures. Mol Cell Biol. 1996; 16:1896–1908. [PubMed: 8628256]

Harlow ML, Ress D, Stoschek A, Marshall RM, McMahan UJ. The architecture of active zone material at the frog's neuromuscular junction. Nature. 2001; 409:479–484. [PubMed: 11206537]

Harzsch S, Miller J, Benton J, Beltz B. From embryo to adult: persistent neurogenesis and apoptotic cell death shape the lobster deutocerebrum. J Neurosci. 1999; 19:3472–3485. [PubMed: 10212307]

Hauser-Holschuh, H. Ph.D. Thesis. Tübingen, Germany: Eberhard-Karls-Universität zu Tübingen; 1975. Vergleichend quantitative Untersuchungen an den Sehganglien der Fliegen *Musca domestica* und *Drosophila melanogaster*.

Hiesinger PR, Scholz M, Meinertzhagen IA, Fischbach K-F, Obermayer K. Visualization of synaptic markers in the optic neuropils of *Drosophila* using a new constrained deconvolution method. J Comp Neurol. 2001; 429:277–288. [PubMed: 11116220]

Hing H, Xiao J, Harden N, Lim L, Zipursky SL. Pak functions downstream of Dock to regulate photoreceptor axon guidance in *Drosophila*. Cell. 1999; 97:853–863. [PubMed: 10399914]

Hinshaw JE. Dynamin and its role in membrane fission. Annu Rev Cell Dev Biol. 2000; 16:483–519. [PubMed: 11031245]

Hofbauer, A. Habilitation-schrift. Würzburg, Germany: University of Würzburg; 1991. Eine Bibliothek monoklonaler Antikörper gegen das Gehirn von *Drosophila melanogaster*.

Hofbauer A, Ebel T, Waltenspiel B, Oswald P, Chen Y-C, Halder P, Biskup S, Lewandrowski U, Winkler C, Sickmann A, Buchner S, Buchner E. The Wuerzburg hybridoma library against *Drosophila* brain. J Neurogenet. 2009; 23:78–91. [PubMed: 19132598]

Ingold AL, Cohn SA, Scholey JM. Inhibition of kinesin-driven microtubule motility by monoclonal antibodies to kinesin heavy chains. J Cell Biol. 1988; 107:2657–2667. [PubMed: 2974459]

Johard HA, Enell LE, Gustafsson E, Trifilieff P, Veenstra JA, Nässel DR. Intrinsic neurons of *Drosophila* mushroom bodies express short neuropeptide F: relations to extrinsic neurons expressing different neurotransmitters. J Comp Neurol. 2008; 507:1479–1496. [PubMed: 18205208]

Kawasaki F, Zou B, Xu X, Ordway RW. Active zone localization of presynaptic calcium channels encoded by the *cacophony* locus of *Drosophila*. J Neurosci. 2004; 24:282–285. [PubMed: 14715960]

Kittel RJ, Wichmann C, Rasse TM, Fouquet W, Schmidt M, Schmid A, Wagh DA, Pawlu C, Kellner RR, Willig KI, Hell SW, Buchner E, Heckmann M, Sigrist SJ. Bruchpilot promotes active zone assembly, Ca^{2+} channel clustering, and vesicle release. Science. 2006; 312:1051–1054. [PubMed: 16614170]

Klagges BRE, Heimbeck G, Godenschwege TA, Hofbauer A, Pflugfelder GO, Reifegerste R, Reisch D, Schaupp M, Buchner S, Buchner E. Invertebrate synapsins: a single gene codes for several isoforms in *Drosophila*. J Neurosci. 1996; 16:3154–3165. [PubMed: 8627354]

Koh TW, Verstreken P, Bellen HJ. Dap160/intersectin acts as a stabilizing scaffold required for synaptic development and vesicle endocytosis. Neuron. 2004; 43:193–205. [PubMed: 15260956]

Kolodziejczyk A, Sun X, Meinertzhagen IA, Nässel DR. Glutamate, GABA and acetylcholine signaling components in the lamina of the fly's visual system. PLoS ONE. 2008; 3:e2110. [PubMed: 18464935]

Koulen P, Fletcher EL, Craven SE, Bredt DS, Wässle H. Immunocytochemical localization of the postsynaptic density protein PSD-95 in the mammalian retina. J Neurosci. 1998; 18:10136–10149. [PubMed: 9822767]

Lahey T, Gorczyca M, Jia XX, Budnik V. The *Drosophila* tumor suppressor gene *dlg* is required for normal synaptic bouton structure. Neuron. 1994; 13:823–835. [PubMed: 7946331]

Lenzi D, Runyeon JW, Crum J, Ellisman MH, Roberts WM. Synaptic vesicle populations in saccular hair cells reconstructed by electron tomography. J Neurosci. 1999; 19:119–132. [PubMed: 9870944]

Lloyd TE, Verstreken P, Ostrin EJ, Phillippi A, Lichtarge O, Bellen HJ. A genome-wide search for synaptic vesicle cycle proteins in *Drosophila*. Neuron. 2000; 26:45–50. [PubMed: 10798391]

Marie B, Sweeney ST, Poskanzer KE, Roos J, Kelly RB, Davis GW. Dap160/intersectin scaffolds the periactive zone to achieve high-fidelity endocytosis and normal synaptic growth. Neuron. 2004; 43:207–219. [PubMed: 15260957]

Mastrogiacomo A, Evans CJ, Gundersen CB. Antipeptide antibodies against a *Torpedo* cysteine-string protein. J Neurochem. 1994; 62:873–880. [PubMed: 8113809]

Meinertzhagen IA. The synaptic populations of the fly's optic neuropil and their dynamic regulation: parallels with the vertebrate retina. Prog Retinal Res. 1993; 12:13–39.

Meinertzhagen IA. Ultrastructure and quantification of synapses in the insect nervous system. J Neurosci Methods. 1996; 69:59–73. [PubMed: 8912936]

Meinertzhagen IA, O'Neil SD. Synaptic organization of columnar elements in the lamina of the wild type in *Drosophila melanogaster*. J Comp Neurol. 1991; 305:232–263. [PubMed: 1902848]

Meinertzhagen IA, Sorra KE. Synaptic organisation in the fly's optic lamina: few cells, many synapses and divergent microcircuits. Prog Brain Res. 2001; 131:53–69. [PubMed: 11420968]

Mentzel B, Raabe T. Phylogenetic and structural analysis of the *Drosophila melanogaster* p21-activated kinase DmPAK3. Gene. 2005; 349:25–33. [PubMed: 15777717]

Muresan V, Lyass A, Schnapp BJ. The kinesin motor KIF3A is a component of the presynaptic ribbon in vertebrate photoreceptors. J Neurosci. 1999; 19:1027–1037. [PubMed: 9920666]

Nicol D, Meinertzhagen IA. Regulation in the number of fly photoreceptor synapses: the effects of alterations in the number of presynaptic cells. J Comp Neurol. 1982; 207:45–60. [PubMed: 7096638]

Nie Z, Ranjan R, Wenniger JJ, Hong SN, Bronk P, Zinsmaier KE. Overexpression of cysteine-string proteins in *Drosophila* reveals interactions with syntaxin. J Neurosci. 1999; 19:10270–10279. [PubMed: 10575024]

Ohtsuka T, Takao-Rikitsu E, Inoue E, Inoue M, Takeuchi M, Matsubara K, Deguchi-Tawarada M, Satoh K, Morimoto K, Nakanishi H, Takai Y. CAST: a novel protein of the cytomatrix at the active zone of synapses that forms a ternary complex with RIM1 and Munc13-1. J Cell Biol. 2002; 158:577–590. [PubMed: 12163476]

Parnas D, Haghighi AP, Fetter RD, Kim SW, Goodman CS. Regulation of postsynaptic structure and protein localization by the Rho-type guanine nucleotide exchange factor dPix. Neuron. 2001; 32:415–424. [PubMed: 11709153]

Parsons TD, Sterling P. Synaptic ribbon: conveyor belt or safety belt? Neuron. 2003; 37:379–382. [PubMed: 12575947]

Peters, A.; Palay, SL.; Webster, H deF. The fine structure of the nervous system. 3rd ed. New York: Oxford University Press; 1991.

Prokop A, Meinertzhagen IA. Development and structure of synaptic contacts in *Drosophila*. Semin Cell Dev Biol. 2006; 17:20–30. [PubMed: 16384719]

Pyza E, Meinertzhagen IA. Circadian rhythms in screening pigment and invaginating organelles in photoreceptor terminals of the housefly's first optic neuropile. J Neurobiol. 1997; 32:517–529. [PubMed: 9110262]

Ready DF, Hanson TE, Benzer S. Development of the *Drosophila* retina, a neurocrystalline lattice. Dev Biol. 1976; 53:217–240. [PubMed: 825400]

Rizo J, Rosenmund C. Synaptic vesicle fusion. Nat Struct Mol Biol. 2008; 15:665–674. [PubMed: 18618940]

Rohrbough J, Rushton E, Woodruff E 3rd, Fergestad T, Vigneswaran K, Broadie K. Presynaptic establishment of the synaptic cleft extracellular matrix is required for post-synaptic differentiation. Genes Dev. 2007; 21:2607–2628. [PubMed: 17901219]

Rosenmund C, Rettig J, Brose N. Molecular mechanisms of active zone function. Curr Opin Neurobiol. 2003; 13:509–519. [PubMed: 14630212]

Schoch S, Gundelfinger ED. Molecular organization of the presynaptic active zone. Cell Tissue Res. 2006; 326:379–391. [PubMed: 16865347]

Shaw SR, Meinertzhagen IA. Evolution of synaptic connections among homologous neurons. Proc Natl Acad Sci U S A. 1986; 83:7961–7965. [PubMed: 3464012]

Sone M, Suzuki E, Hoshino M, Hou D, Kuromi H, Fukata M, Kuroda S, Kaibuchi K, Nabeshima Y-I, Hama C. Synaptic development is controlled in the periactive zones of *Drosophila* synapses. Development. 2000; 127:4157–4168. [PubMed: 10976048]

Stark WS, Carlson SD. Ultrastructure of capitate projections in the optic neuropil of Diptera. Cell Tissue Res. 1986; 246:481–486. [PubMed: 3098431]

Sterling P, Matthews G. Structure and function of ribbon synapses. Trends Neurosci. 2005; 28:20–29. [PubMed: 15626493]

Stowers RS, Megeath LJ, Górska-Andrzejak J, Meinertzhagen IA, Schwarz TL. Axonal transport of mitochondria to synapses depends on Milton, a novel *Drosophila* protein. Neuron. 2002; 36:1063–1077. [PubMed: 12495622]

Stuart AE, Borycz J, Meinertzhagen IA. The dynamics of signaling at the histaminergic photoreceptor synapse of arthropods. Prog Neurobiol. 2007; 82:202–227. [PubMed: 17531368]

Südhof TC. The synaptic vesicle cycle: a cascade of protein-protein interactions. Nature. 1995; 375:645–653. [PubMed: 7791897]

Südhof TC. The synaptic vesicle cycle. Annu Rev Neurosci. 2004; 27:509–547. [PubMed: 15217342]

Südhof TC, Czernik AJ, Kao H-T, Takei K, Johnston PA, Horiuchi A, Kanazir SD, Wagner MA, Perin MS, DeCamilli P, Greengard P. Synapsins: mosaics of shared and individual domains in a family of synaptic vesicle phosphoproteins. Science. 1989; 245:1474–1480. [PubMed: 2506642]

Takao-Rikitsu E, Mochida S, Inoue E, Deguchi-Tawarada M, Inoue M, Ohtsuka T, Takai Y. Physical and functional interaction of the active zone proteins, CAST, RIM1, and Bassoon, in neurotransmitter release. J Cell Biol. 2004; 164:301–311. [PubMed: 14734538]

Tejedor FJ, Bokhari A, Rogero O, Gorczyca M, Zhang J, Kim E, Sheng M, Budnik V. Essential role for *dlg* in synaptic clustering of Shaker K^+ channels *in vivo*. J Neurosci. 1997; 17:152–159. [PubMed: 8987744]

Thomas U, Kim E, Kuhlendahl S, Koh YH, Gundelfinger ED, Sheng M, Garner CC, Budnik V. Synaptic clustering of the cell adhesion molecule fasciclin II by discs-large and its role in the regulation of presynaptic structure. Neuron. 1997; 19:787–799. [PubMed: 9354326]

tom Dieck S, Sanmartí-Vila L, Langnaese K, Richter K, Kindler S, Soyke A, Wex H, Smalla KH, Kämpf U, Fränzer JT, Stumm M, Garner CC, Gundelfinger ED. Bassoon, a novel zincfinger CAG/glutamine-repeat protein selectively localized at the active zone of presynaptic nerve terminals. J Cell Biol. 1998; 142:499–509. [PubMed: 9679147]

tom Dieck S, Altrock WD, Kessels MM, Qualmann B, Regus H, Brauner D, Fejtová A, Bracko O, Gundelfinger ED, Brandstätter JH. Molecular dissection of the photoreceptor ribbon synapse: physical interaction of Bassoon and RIBEYE is essential for the assembly of the ribbon complex. J Cell Biol. 2005; 168:825–836. [PubMed: 15728193]

Verhage M, Toonen RF. Regulated exocytosis: merging ideas on fusing membranes. Curr Opin Cell Biol. 2007; 19:402–408. [PubMed: 17629692]

Wagh DA, Rasse TM, Asan E, Hofbauer A, Schwenkert I, Dürrbeck H, Buchner S, Dabauvalle M-C, Schmidt M, Qin G, Wichmann C, Kittel R, Sigrist SJ, Buchner E. Bruchpilot, a protein with homology to ELKS/CAST, is required for structural integrity and function of synaptic active zones in *Drosophila*. Neuron. 2006; 49:833–844. [PubMed: 16543132]

Wang Y, Okamoto M, Schmitz F, Hofmann K, Sudhof TC. Rim is a putative Rab3 effector in regulating synaptic-vesicle fusion. Nature. 1997; 388:593–598. [PubMed: 9252191]

Wang Y, Sugita S, Sudhof TC. The RIM/NIM family of neuronal C2 domain proteins—interactions with Rab3 and a new class of Src homology 3 domain proteins. J Biol Chem. 2000; 275:20033–20044. [PubMed: 10748113]

Wang Y, Liu XR, Biederer T, Sudhof TC. A family of RIM-binding proteins regulated by alternative splicing: implications for the genesis of synaptic active zones. Proc Natl Acad Sci U S A. 2002; 99:14464–14469. [PubMed: 12391317]

Wang XL, Kibschull M, Laue MM, Lichte B, Petrasch-Parwez E, Kilimann MW. Aczonin, a 550-kD putative scaffolding protein of presynaptic active zones, shares homology regions with rim and bassoon and binds profiling. J Cell Biol. 1999; 147:151–162. [PubMed: 10508862]

Woods DF, Bryant PJ. ZO-1, DlgA and PSD-95/SAP90: homologous proteins in tight, septate and synaptic cell junctions. Mech Dev. 1993; 44:85–89. [PubMed: 8155583]

Woods DF, Hough C, Peel D, Callaini G, Bryant PJ. Dlg protein is required for junction structure, cell polarity, and proliferation control in *Drosophila* epithelia. J Cell Biol. 1996; 134:1469–1482. [PubMed: 8830775]

Zhai RG, Bellen HJ. The architecture of the active zone in the presynaptic nerve terminal. Physiology. 2004; 19:262–270. [PubMed: 15381754]

Zinsmaier KE, Hofbauer A, Heimbeck G, Pflugfelder GO, Buchner S, Buchner E. A cysteine-string protein is expressed in retina and brain of *Drosophila*. J Neurogenet. 1990; 7:15–29. [PubMed: 2129171]

Zinsmaier KE, Eberle KK, Buchner E, Walter N, Benzer S. Paralysis and early death in cysteine string protein mutants of *Drosophila*. Science. 1994; 263:977–980. [PubMed: 8310297]

Zito K, Fetter RD, Goodman CS, Isacoff EY. Synaptic clustering of Fasciclin II and Shaker: essential targeting sequences and role of Dlg. Neuron. 1997; 19:1007–1016. [PubMed: 9390515]

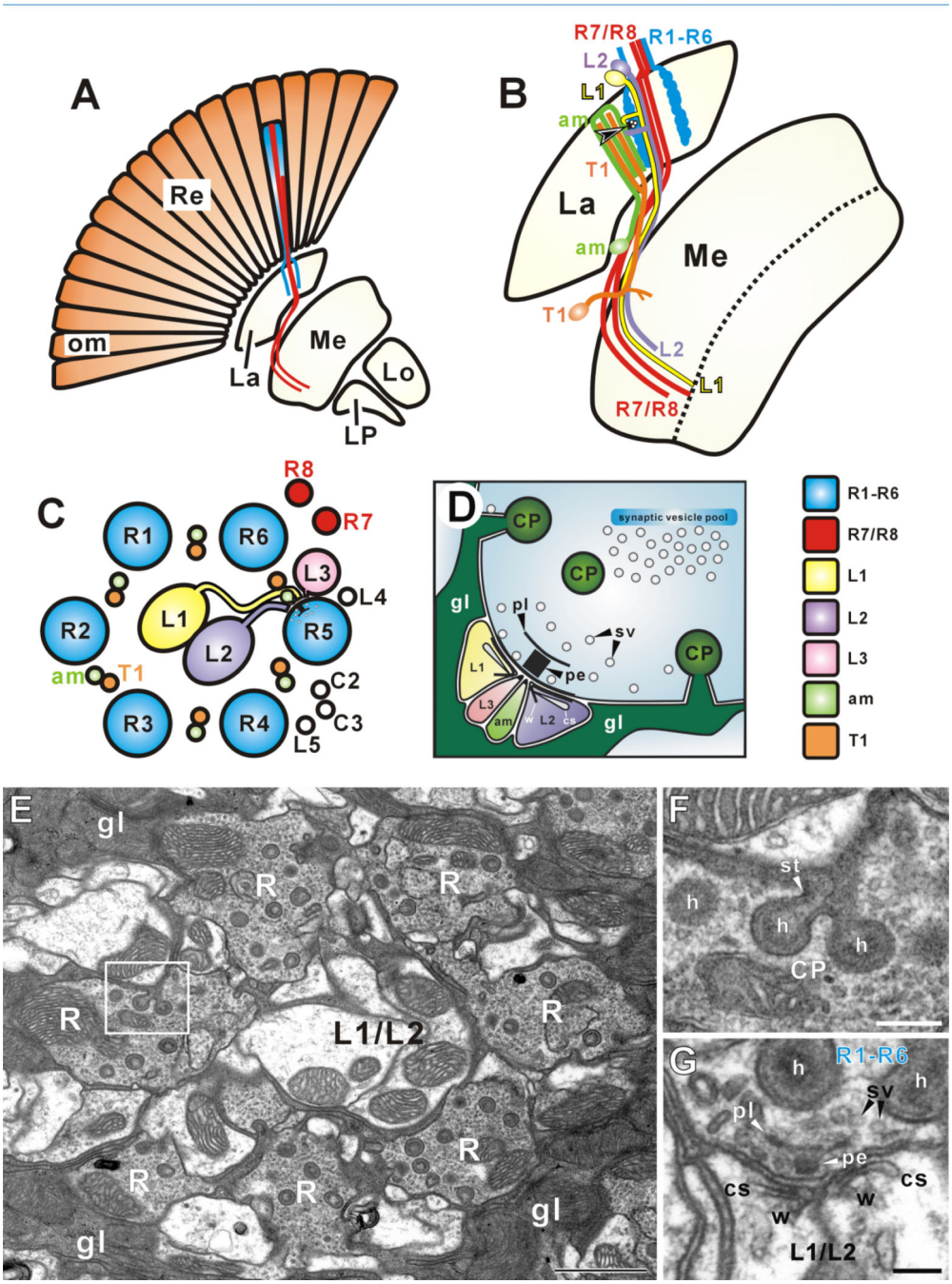

Figure 1.

Synaptic connections in the lamina. **A**: The retina (Re) is arrayed as about 750 ommatidia (om), each containing eight photoreceptor cell neurons (R1–R8) (Ready et al., 1976). These are of two types, an outer set of six (R1–R6), which innervate the lamina (La), establishing an array of cartridges that corresponds to the array of ommatidia, and an inner pair (R7 and R8), which terminate in the second neuropil, the medulla (Me). The lobula (Lo) and lobula plate (LP) in turn lie central to these. R1–R6 of each ommatidium sort into adjacent cartridges in the lamina. **B**: R1–R6 terminals provide input to the dendrites of second-order

interneurons with cell bodies in the overlying cortex. Shown are L1 (yellow) and L2 (purple), and amacrine (am, light green) cells, but additional cells such as T1 (orange) also exist. Clusters of four postsynaptic elements establish a tetrad at each presynaptic site (arrowhead). They invariably contain L1 and L2, and two other contributions from a local amacrine cell, an L3 cell, and/or epithelial glia (Nicol and Meinertzhagen, 1982). **C**: Cartridge cross section. The ring of R1–R6 photoreceptor terminals surrounds the axons of L1 and L2, separated by paired neurites of amacrine (am) and T1 cells, and other interneurons (L4, L5, C2, and C3). Axons of R7 and R8 run alongside the cartridge. Processes from L1 and L2, usually as paired spines, combine with those from amacrine and L3 cells to form a common postsynaptic cluster. **D**: Photoreceptor tetrad synapse revealed by electron-dense presynaptic T-bar ribbon, comprising a platform (pl) surmounting a pedestal (pe) with nearby synaptic vesicles (sv). Capitate projections (CPs) from epithelial glia (gl) invaginate nearby. Postsynaptic sites in L1 and L2 are marked by postsynaptic cisternae (cs) and protein whisker filaments (w) linking the cisterna to postsynaptic membrane (Burkhardt and Braitenberg, 1976). **E**: Electron micrograph of single cartridge surrounded by epithelial glia (gl). Compare details with C. **F**: Enlarged image of rectangle in E showing epithelial glia invaginating at capitate projections (CPs), that comprise a 190-nm-diameter head (h) and stalk (st). **G**: Photoreceptor terminal (R1–R6) synapse upon L1 and L2 spines (compare details with D). Capitate projection head (h) approaches within 100 nm of tetrad ribbon decorated with synaptic vesicles (sv). Scale bar = 1 μm in E; 200 nm in F; 100 nm in G.

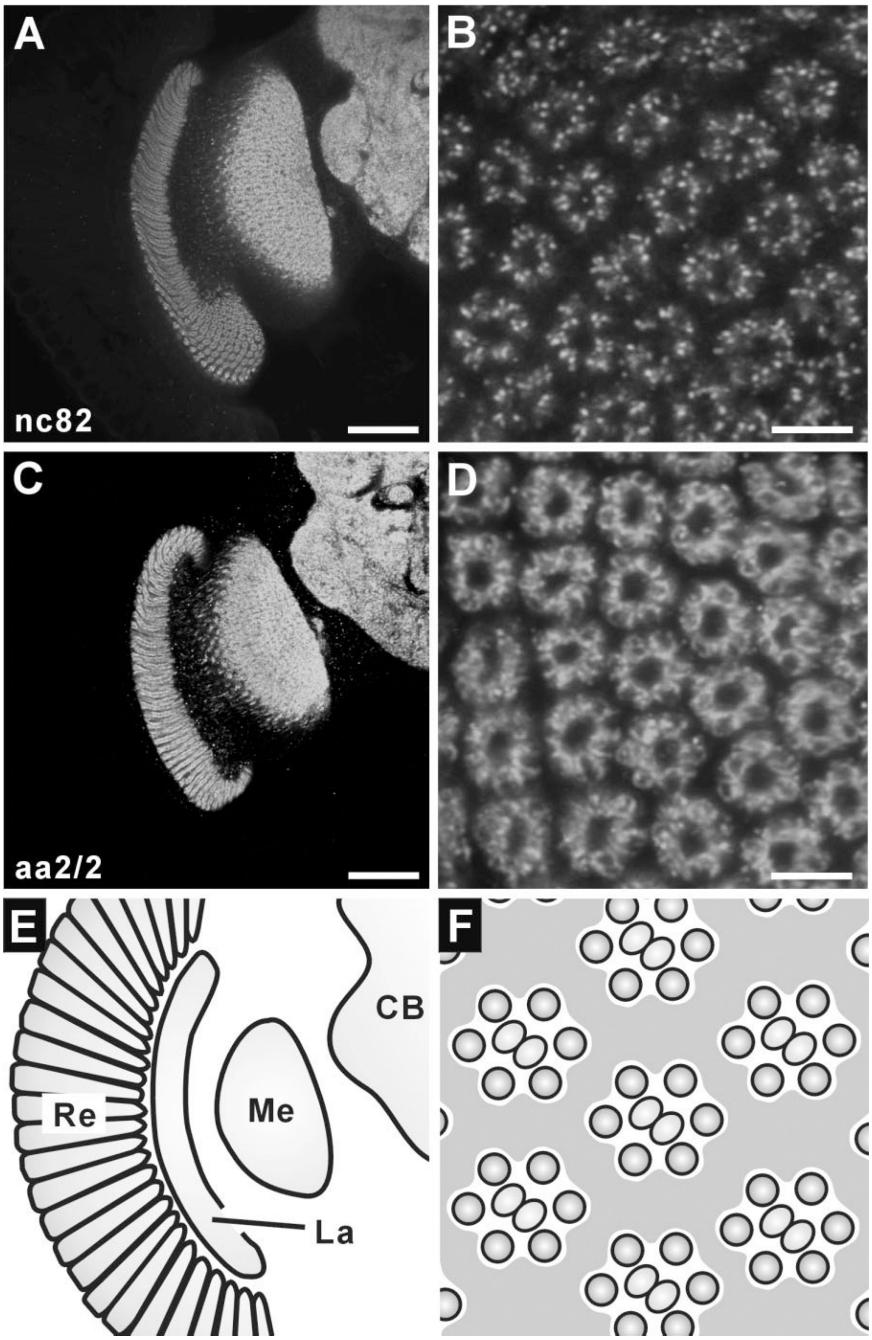

Figure 2.

Immunoreactivity to nc82 (anti-BRP; A,B) and aa2/2 (anti-EPS-15; C,D) in the *Drosophila* optic lobe. Single confocal sections in frontal views of the optic lobe (A,C; dorsal to the top and medial to the right), and corresponding lamina cross sections (B,D). **A**: Anti-BRP (nc82) strongly labels both the lamina and medulla as well as central brain neuropils. **B**: In cross-sectioned lamina cartridges, immunonoreactive signals comprise numerous puncta mostly in an outer ring containing R1–R6 terminals. **C**: Anti-EPS-15 (aa2/2) clearly labels the lamina, medulla, and central brain neuropils, but not the overlying retina. **D**:

Immunoreactive outlines of photoreceptor terminals, with the strongest signals lining sites that face the cartridge center. **E**: Schematic diagram of a right optic lobe having the same orientation as A and C, and also as panels in left columns of Figures 3 and 4. **F:** Schematic diagram of cross-sectioned lamina for comparison with B and D, and also with panels in right columns of Figures 3 and 4. CB, central brain. La, lamina; Me, medulla; Re, retina. Scale bar = 50 μm in A,C; 5 μm in B,D.

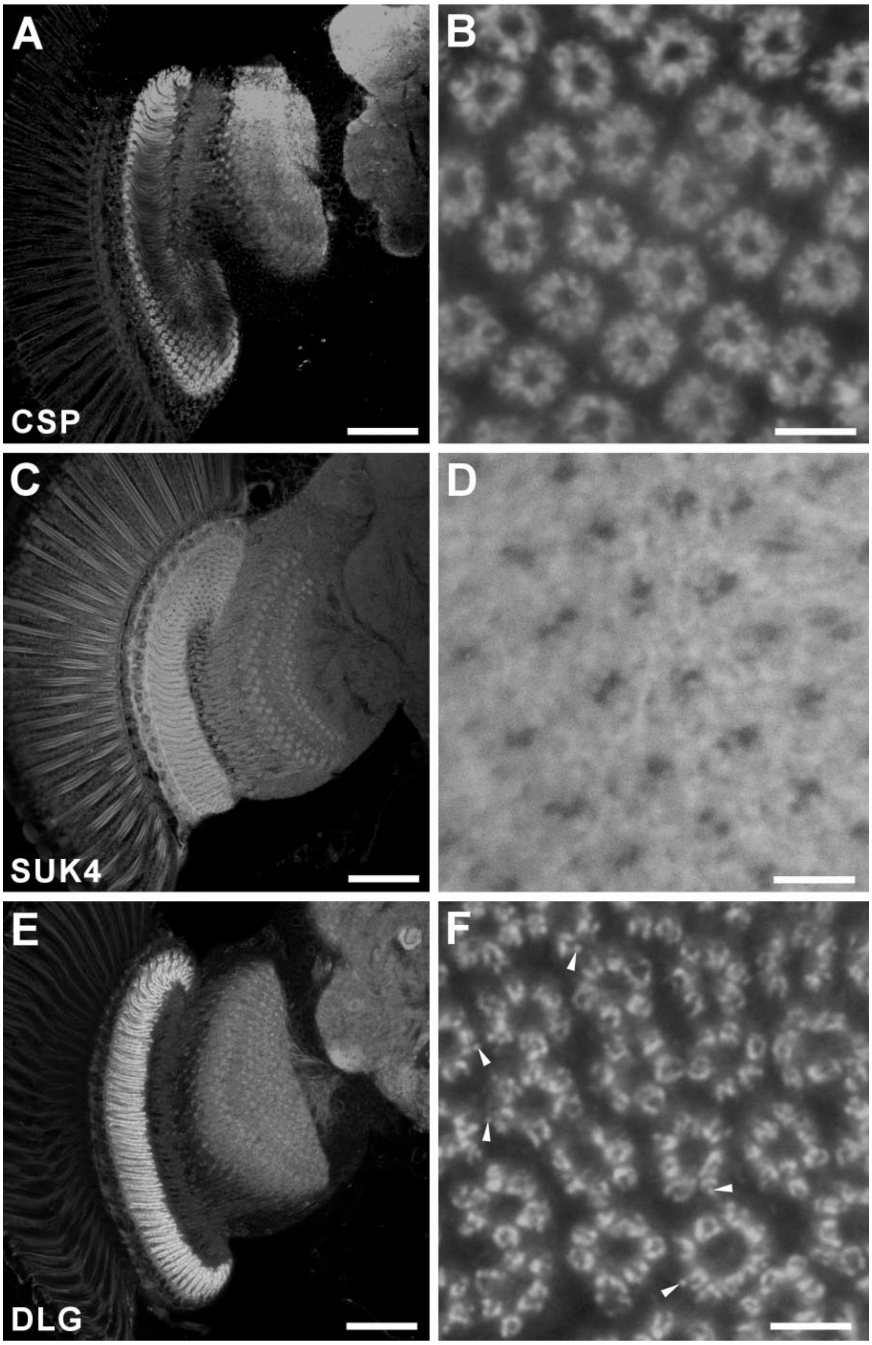

Figure 3.

Immunolabeling of CSP (A,B), kinesin with antibody SUK4 (C,D) and DLG (E,F) in single confocal sections of the *Drosophila* optic lobe. A,C,E: Frontal plane (dorsal to the top, medial to the right). B,D,F: Corresponding lamina cross sections. **A:** Anti-CSP strongly labels the lamina, and other neuropils as well. The penetration of this antibody is restricted, leading to the reduced signal in central regions of the lamina. **B:** Immuno-reactive signal is localized within the photoreceptor terminals mostly to the faces lining the center of cartridge, where many tetrads are located, but with some cytoplasmic signal also visible. **C:**

Anti-kinesin (SUK4) labels the lamina neuropil less strongly than nc82, whereas the medulla and central brain neuropils are hardly labeled. **D:** SUK4 signals in the lamina are weak and diffuse compared with nc82 immunolabeling. Glial cells surrounding the lamina terminals of R1–R6 are also labeled. **E:** Anti-DLG antibody strongly labels the neuropil in the lamina, but less strongly the medulla and central brain. **F:** In the lamina, anti-DLG labeling clearly reveals the round profiles of R1–R6 terminals, but these are ring-shaped with dark lacunae. Some immunoreactive substructures are visible as spots or puncta (arrowheads). Scale bar = 50 μm in A,C,E; 5 μm in B,D,F.

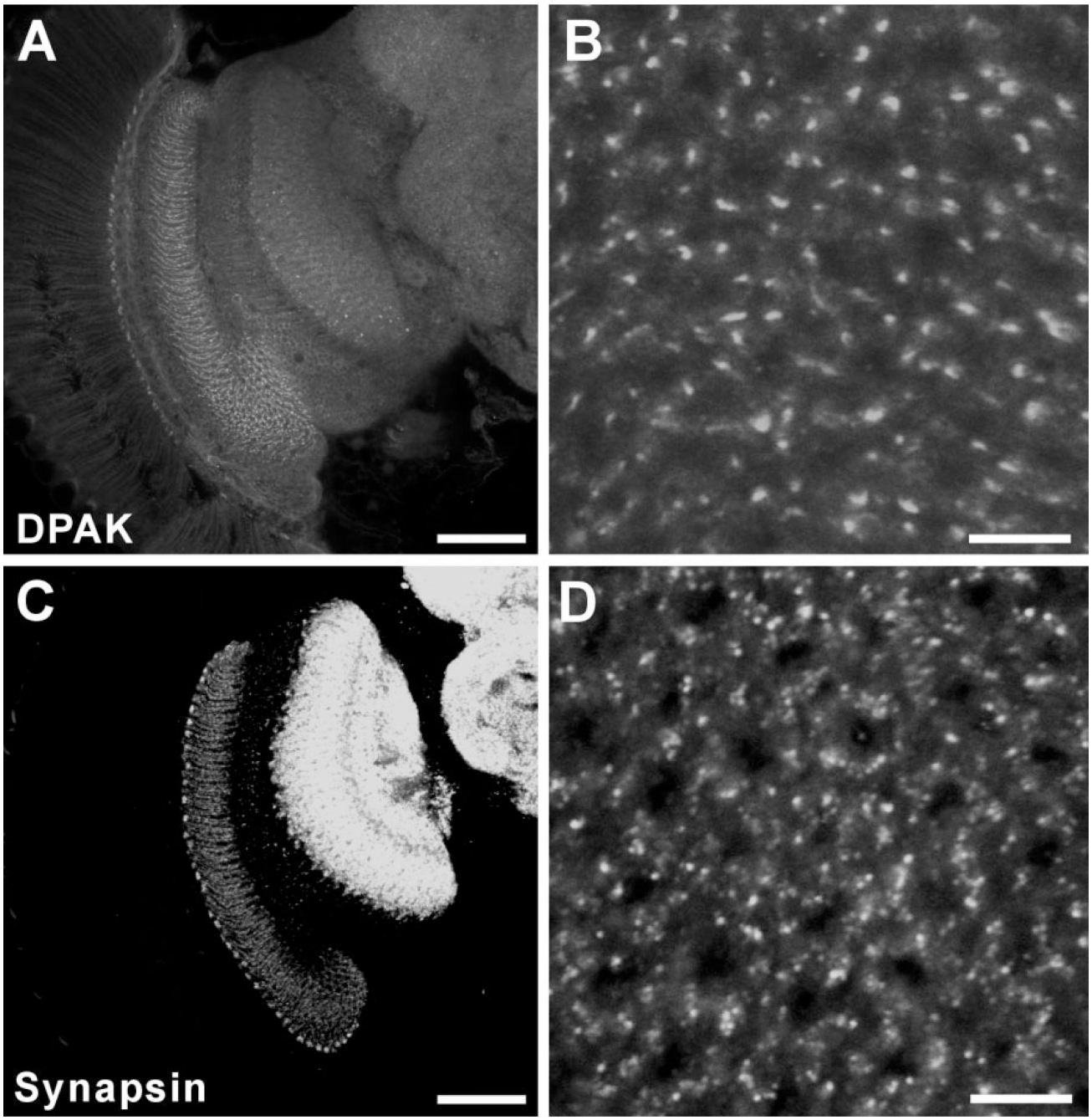

Figure 4.

Immunolabeling with anti-DPAK (A,B) and anti-synapsin (C,D) in the *Drosophila* optic lobe. All images are single confocal sections. A,C: Frontal view of the optic lobe (dorsal to the top and medial to the right). B,D: Cross-sectional views of the lamina neuropil. **A:** Anti-DPAK hardly labeled neuropils in the medulla and central brain. The small dot-like signals were restricted to the lamina. **B:** Anti-DPAK labeled restricted regions in the lamina and the signals showed punctate distribution. **C:** Anti-synapsin labeled neuropils in the lamina, medulla, and central brain. Signals in medulla and central brain neuropils were stronger than

those in the lamina. **D:** In cross sections, the signals in the lamina showed punctate distribution but did not reveal as clear cartridge structures as nc82. Scale bar = 50 μm in A,C; 5 μm in B,D.

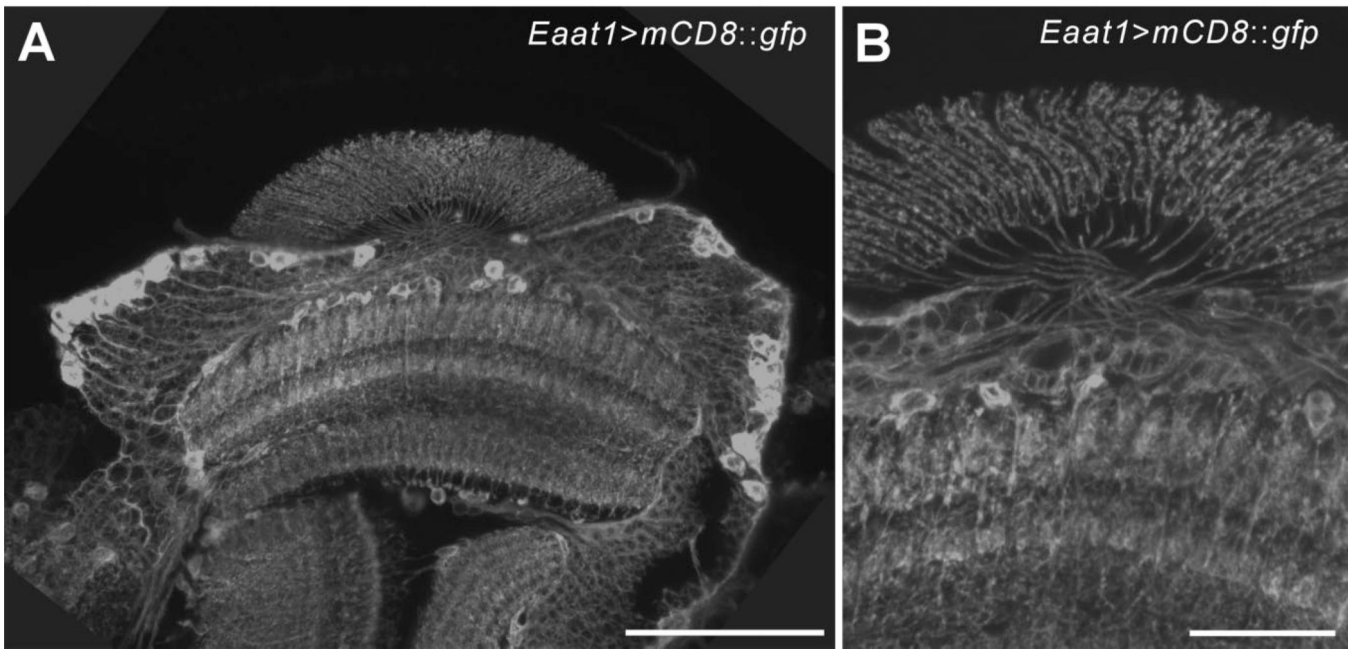

Figure 5.

T1 cells visualized by *Eaat1* -GAL4-driven mCD8::GFP expression. A,B: Horizontal confocal stacks of 8 (A) and 3 (B) optical slices of lamina R1–R6 terminals, captured at 1-μm intervals. GFP expression was enhanced by immunolabeling with anti-GFP. The anti-GFP labeled many cell bodies in the medulla cortex the axons of which extend toward the lamina neuropil, cross in the outer chiasm, and penetrate the lamina neuropil (**A**), to form basket-shaped terminal arborizations typical of T1 cells (**B**). Scale bar = 50 μm in A; 20 μm in B.

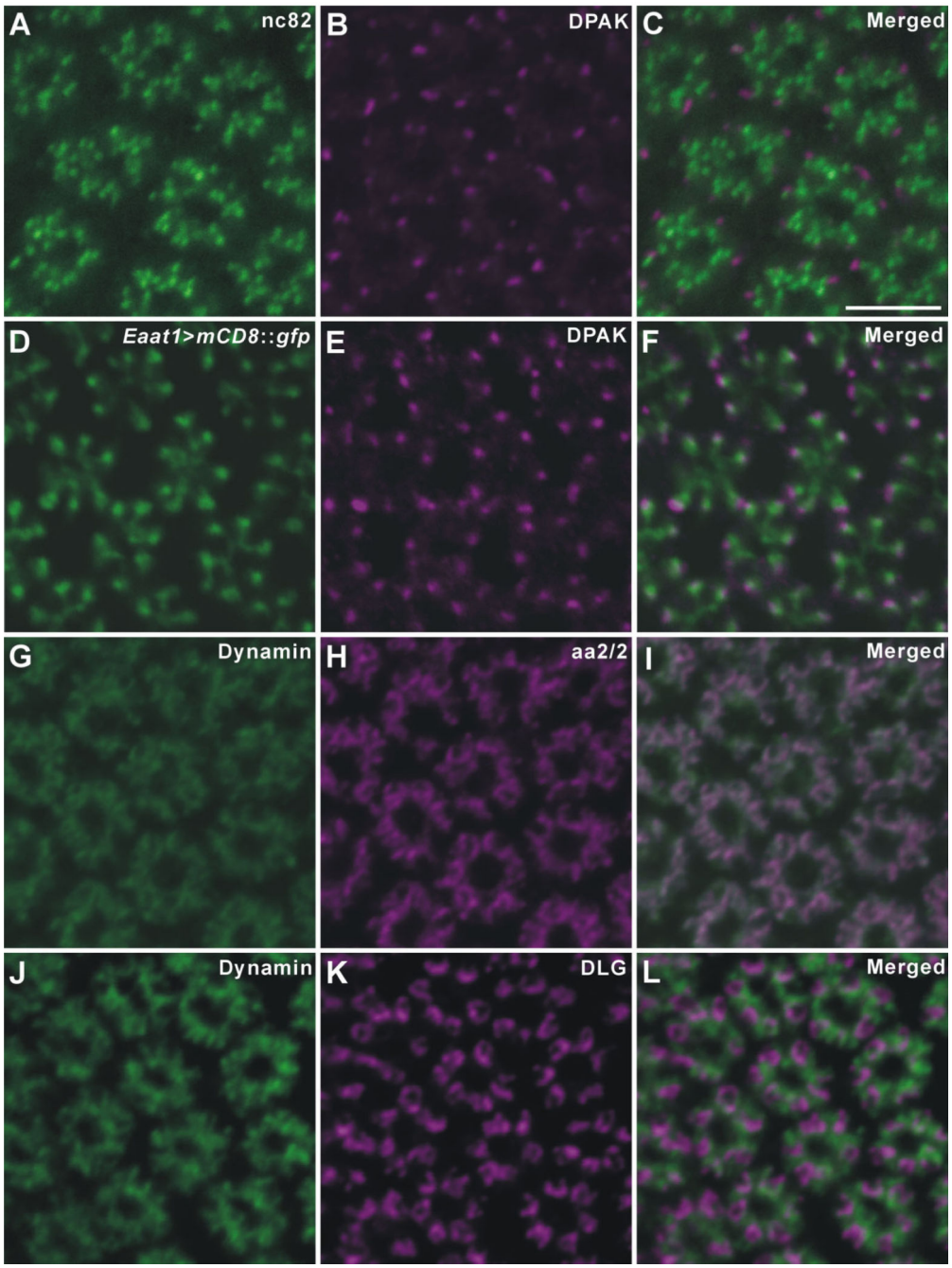

Figure 6.

Drosophila R1–R6 terminals in the lamina double-immunolabeled with anti-DPAK (B,E), and either nc82, anti-BRP (A), or *Eaat1* -GAL4-driven GFP expression (D); or with anti-dynamin (G,J) and either aa2/2, anti-EPS-15 (H), or anti-DLG (K). C,F,I,L: Corresponding merged images. All are single 1-μm-thick confocal crossed sections. **A–C:** Both signals concentrate in an area conforming to the ring of R1–R6 terminals; anti-DPAK immunopuncta (magenta) lie close to the more numerous anti-BRP puncta (green), but without overlap, whereas such puncta often overlap the distal tips of the basket endings of

the T1 cells labeled by *Eaat1* -GAL4-driven GFP expression (**F**). GFP signals are enhanced by anti-GFP as in images in fFigure 5. **G–I:** Dynamin (green) and EPS-15 (aa2/2: magenta) almost completely co-localize in the cytoplasm of R1–R6 terminals. **J–L:** Anti-Dynamin (green) and anti-DLG (magenta) signals show a complementary pattern of distribution in R1–R6 terminals, with the Dynamin expression surrounding DLG expression. Scale bar =5 μm in C (applies to A–L).

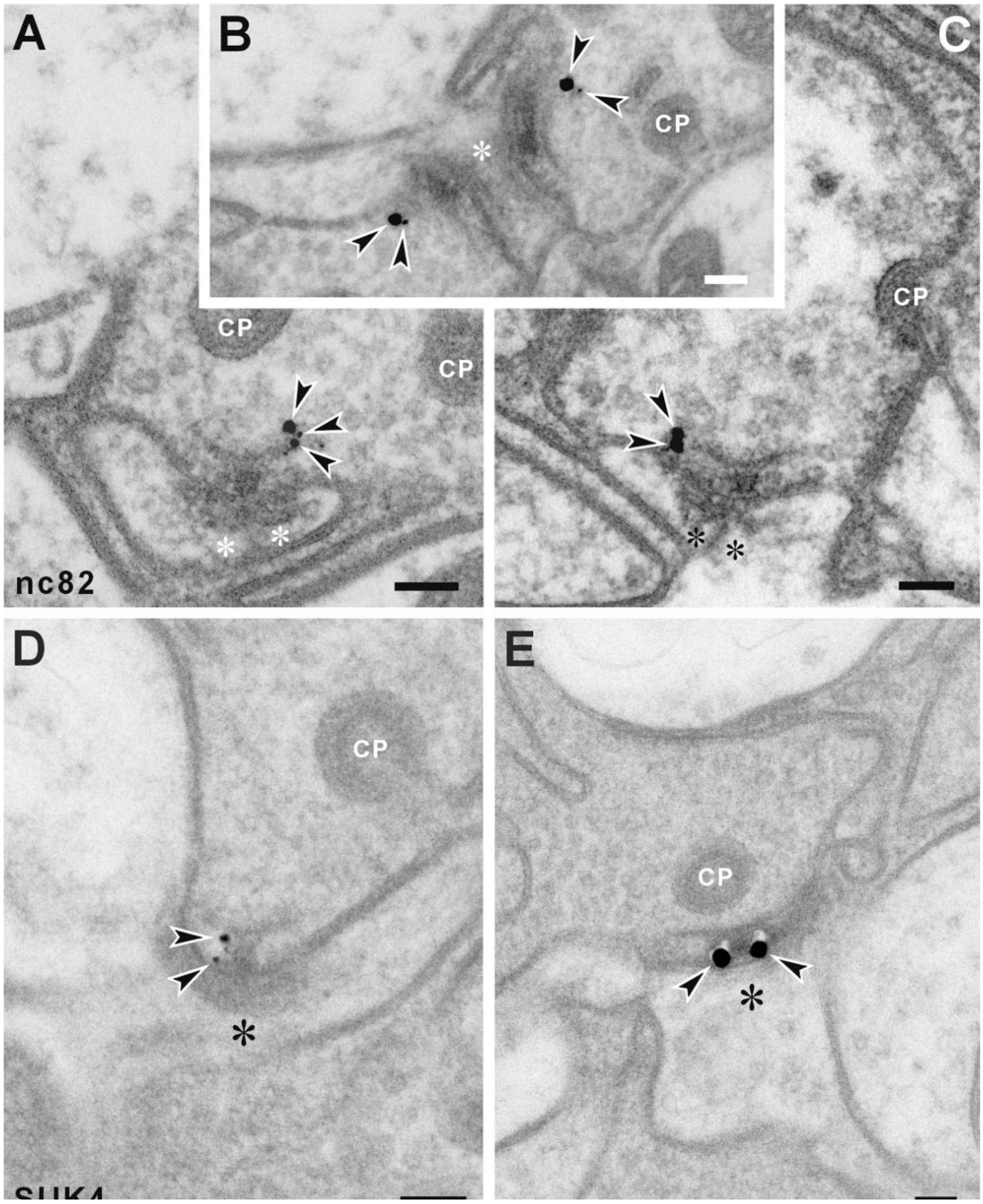

Figure 7.

Immuno-EM subcellular localization of anti-BRP (nc82) binding (A–C), and anti-kinesin heavy chain (SUK4) binding (D,E), in the lamina terminals of *Drosophila* R1–R6. **A–C:** Anti-BRP (nc82) signals localize to the edge of the platform, but neither to other regions of the platform nor, in particular, to the pedestal. **D,E:** Anti-kinesin (SUK4) signals localize at sites reciprocal to those of anti-BRP, close to the pedestal of the T-bar ribbon, but not to its platform. Arrowheads, silver-enhanced gold particles; asterisks, postsynaptic profiles of either L1 or L2. CP, capitate projection head. Scale bar = 100 nm in A–E.

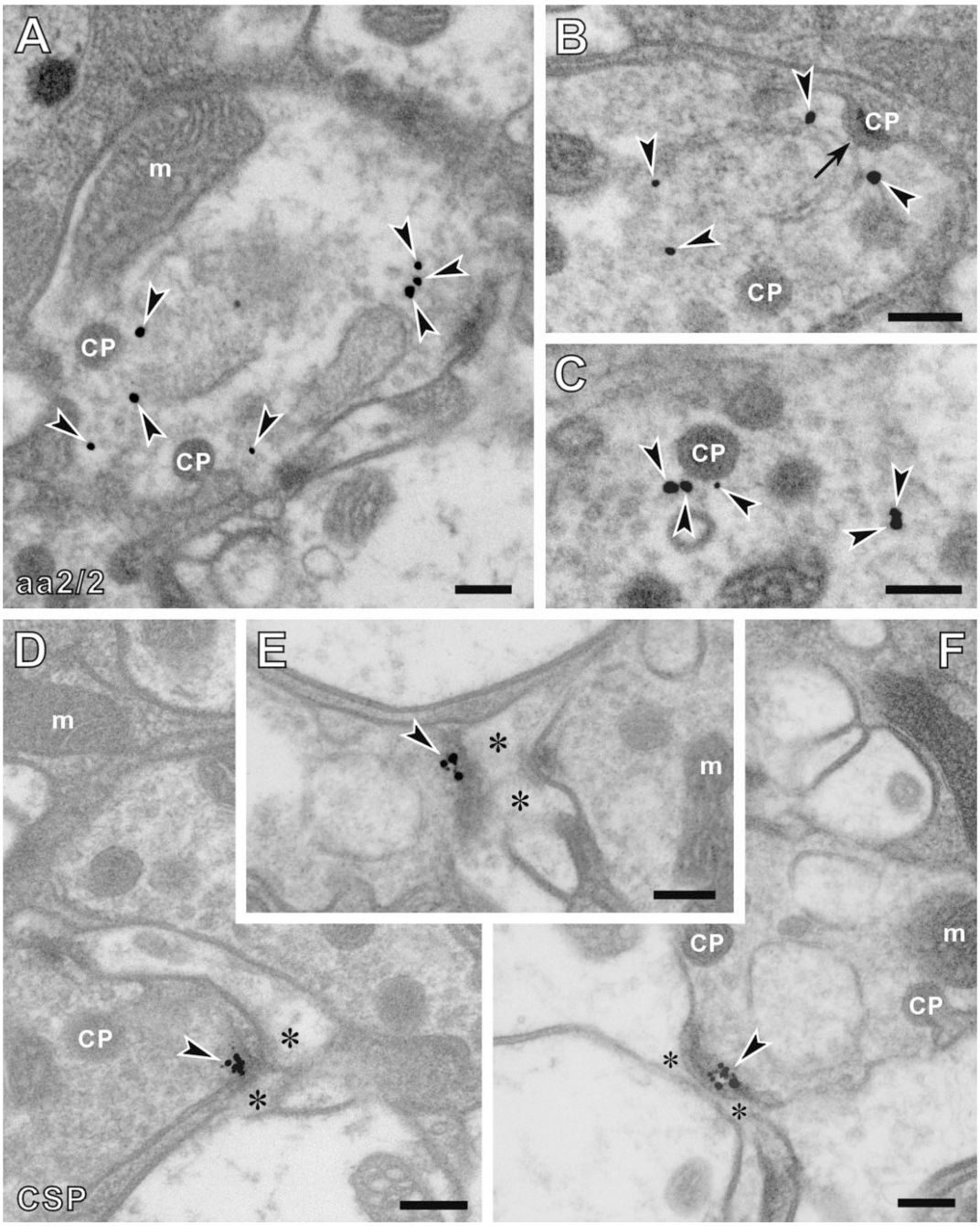

Figure 8.

Immuno-EM subcellular location of anti-EPS-15, aa2/2 (A–C), and anti-CSP (D–F) signals in the R1–R6 terminals of *Drosophila* photoreceptors. **A–C:** Anti-EPS-15 (aa2/2) signals were located in the synaptic vesicle pool of photoreceptor cells close to the heads of capitate projections (CPs). At some sites, signal was seen close to the shallow forms of these organelles (arrow in B), which are thought to be sites of either invagination or retraction of the deep, penetrating capitate projections. **D–F:** Anti-CSP signals were detected at the

presynaptic T-bar ribbons decorated with synaptic vesicles. Arrowheads, silver-enhanced gold particles; asterisks, postsynaptic profiles. m, mitochondria. Scale bar= 200 nm in A–F.

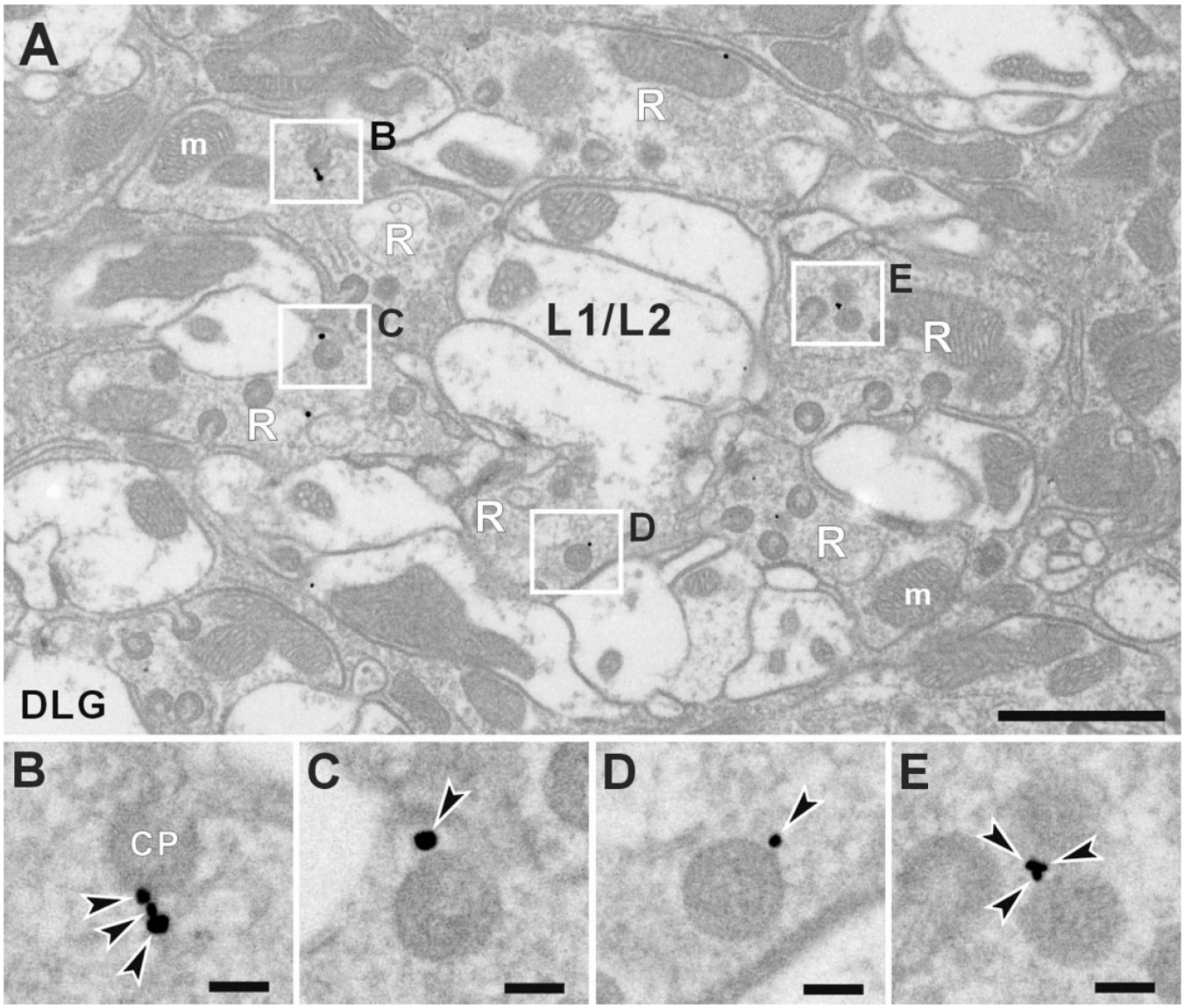

Figure 9.

Immuno-EM subcellular location of anti-DLG binding in the R1–R6 terminals of *Drosophila* photoreceptors. **A:** Cross section of a lamina cartridge with four sites of immunolabeling outlined. **B–E:** Enlarged images of rectangles in A. Within the terminal, anti-DLG signals localize sharply to the invaginating head of the capitate projections (CP), which are invaginations from surrounding glia and specialized organelles often occurring close to the T-bar ribbon. Signals were not seen in the stalk of capitate projections. Arrowheads indicate silver-enhanced gold particles. m, mitochondria; R, photoreceptor terminals; L1/L2, axons of L1 and L2 cells. Scale bar = 1 μm in A; 100 nm in B–E.

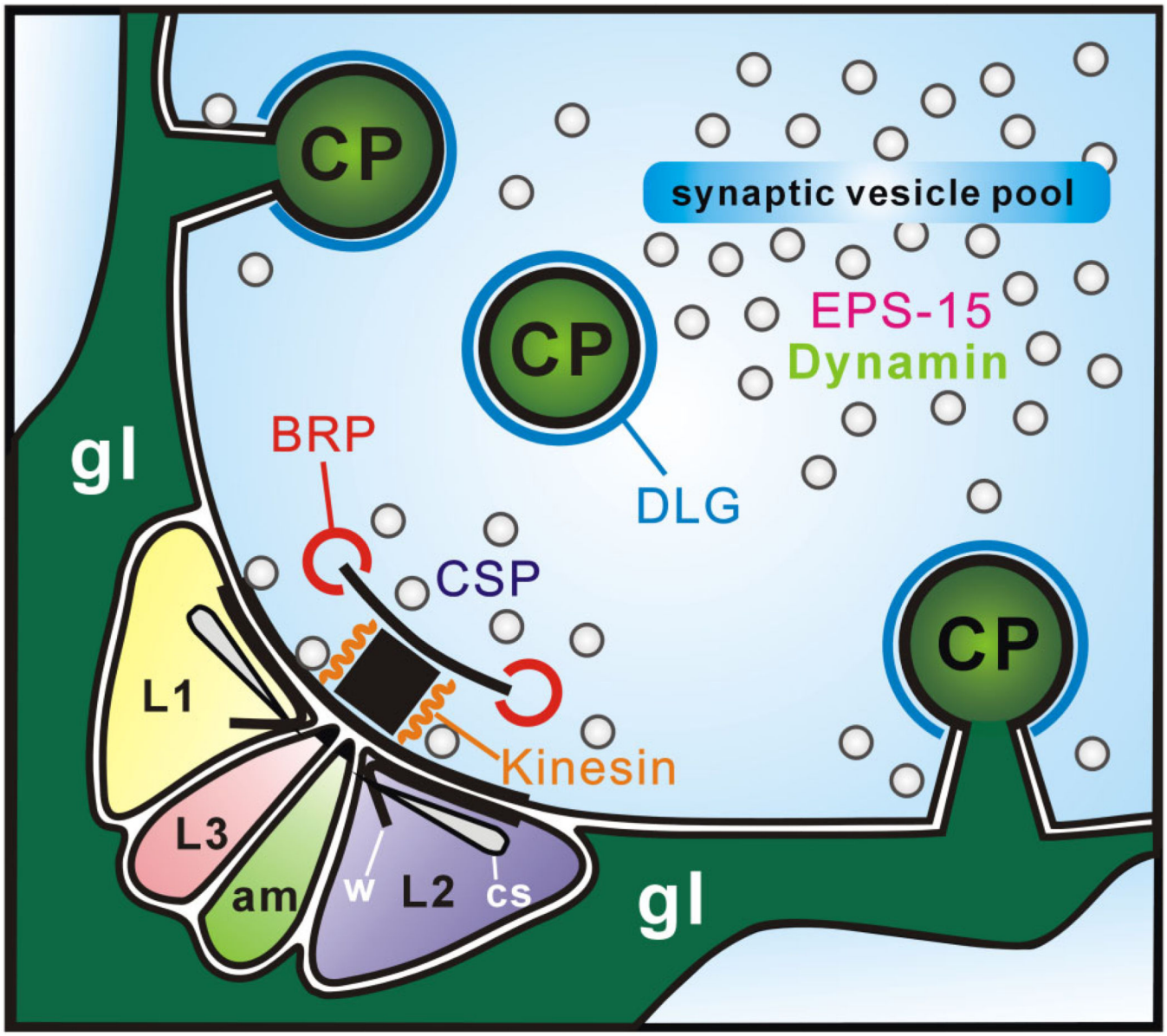

Figure 10.

Subcellular locations of synaptic proteins relative to the synaptic organelles of tetrad synapses in *Drosophila* R1–R6 terminals. Two epitopes are located on the T-bar ribbon: those recognized by anti-BRP (nc82) at the edge of the platform, and by anti-kinesin (SUK4) close to its pedestal. Three epitopes are located among the vesicle pool surrounding the tetrad release site: *Drosophila* EPS-15 (aa2/2 antigen) and Dynamin in the synaptic vesicle pool itself surrounding sites of endocytosis, capitate projections (CPs), and cysteine string protein (CSP) close to the presynaptic membrane decorated with synaptic vesicles. A sixth synaptic epitope, Discs large (DLG), is localized to the heads of capitate projections close to the T-bar ribbon. am, amacrine cell; cs, cisternae; gl, epithelial glia; w, whisker.

TABLE 1

Primary Antibodies Used

Antibody	Working dilution	Source of or reference to antibody	Immunogen
aa2/2	1:20 (LM), 1:50 (EM)	Dr. E. Buchner (Würzburg, Germany)	*Drosophila* head homogenate
Anti-CSP	1:25 (LM), 1:100 (EM)	Dr. K.E. Zinsmaier (Tucson, AZ)	*Drosophila* head homogenate
Anti-DLG	1:50 (LM), 1:100 (EM)	DSHB, Iowa City, IA	DLG PDZ2 domain fused to GST
Anti-DPAK	1:2,000 (LM), 1:200 (EM)	Harden et al., 1996	N-terminal DPAK fused to GST
Anti-Dynamin	1:200 (LM)	Estes et al., 1996	66-kDa fragment of *Drosophila* dynamin fused to MBP
Anti-synapsin	1:25 (LM), 1:25 (EM)	Dr. E. Buchner (Würzburg) or DSHB	Synapsin protein fused to GST
nc82	1:10 (LM), 1:50 (EM)	Dr. E. Buchner (Würzburg) or DSHB	*Drosophila* head homogenate
SUK4	1:20 (LM), 1:50 (EM)	DSHB	130-kDa heavy chain of sea urchin egg kinesin

Abbreviations: EM, electron microscopy; GST, glutathione-S-transferase; LM, light microscopy; MBP, maltose-binding protein. For other abbreviations, see list.